

Retrospective Experience with Medullary Thyroid Carcinoma

Farrah L. Harden, B.S., Amy R. Quillo, M.D., Elsa T. Stephen, B.A., Kelsey E. Lewis, B.S., Michael B. Flynn, M.D., Jeffrey M. Bumpous, M.D., Richard E. Goldstein, M.D. Ph.D., Robert C. G. Martin, II M.D. Ph. D., Glenda G. Callender, M.D.

Department of Surgery
University of Louisville School of Medicine

◆ Introduction

Medullary Thyroid Carcinoma (MTC) is a relatively rare cancer that occurs both sporadically and in the setting of inherited *RET* protooncogene mutations associated with Multiple Endocrine Neoplasia Type 2. Our goal was to review our local experience with MTC.

◆ Methods & Materials

A retrospective study was performed of all patients undergoing thyroidectomy for a diagnosis of thyroid cancer in a single institution from 01/01/2001-12/31/2011. Charts were reviewed for demographic variables, operative notes, pathology reports, and biochemical data.

◆ Results

A total of 352 patients were identified who underwent thyroidectomy for thyroid cancer. Of these, 14 (4%) patients had a diagnosis of MTC. All but one patient underwent initial thyroidectomy at our high-volume thyroid center; that patient underwent thyroid lobectomy in the community for a thyroid nodule and was referred for further management once the diagnosis of MTC was made. One patient underwent thyroid lobectomy at our center for unilateral goiter; when MTC was diagnosed on final pathology, the patient did not follow up for additional surgical management. One patient underwent prophylactic thyroidectomy for known MEN2A; the remainder of the patients underwent therapeutic thyroidectomy and appropriate lymph node dissection. Results of genetic testing for MEN2 were available for 5 patients; 4 tested positive for MEN2A and 1 tested negative.

◆ Images



Figure 1- Gross pathology of two thyroid specimens with MTC. Tumors tend to develop in the superior and posterior aspect of the thyroid, in the location of embryonic migration of the c-cells.

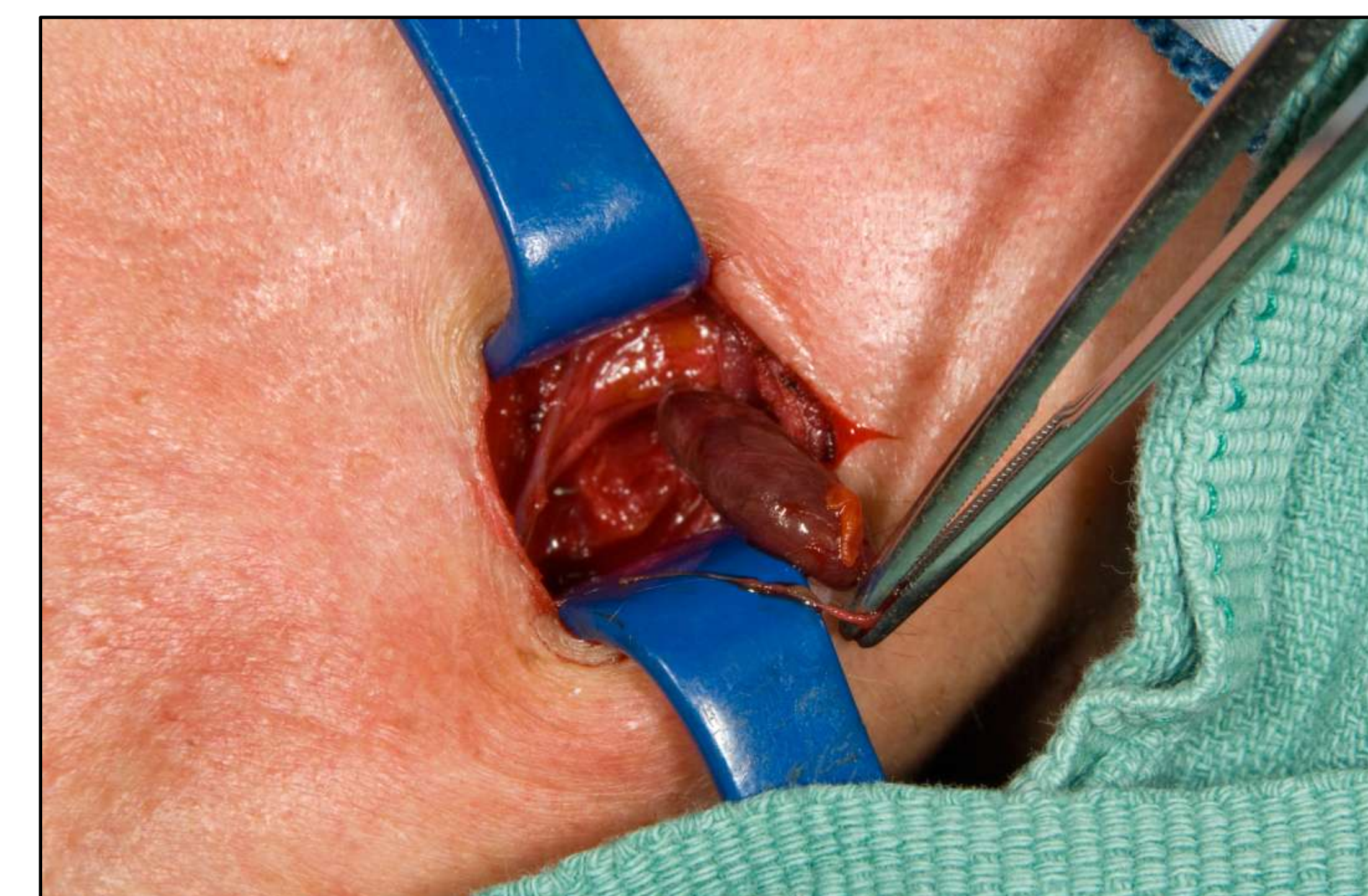


Figure 2- Resection of an enlarged parathyroid gland. Primary hyperparathyroidism is one of the prominent symptoms common to MEN2A patients.

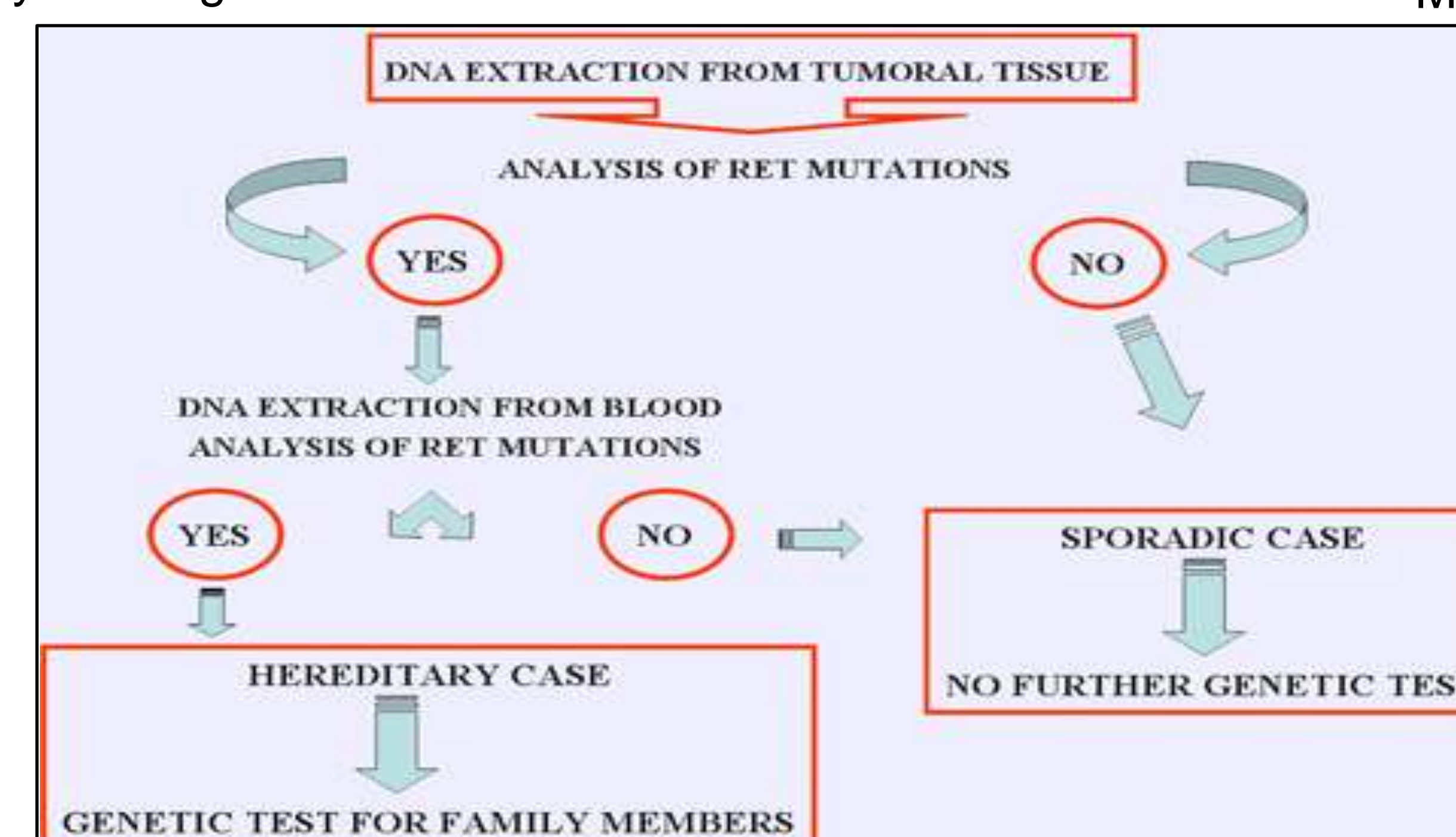


Figure 3-Algorithm for genetic screening in apparently sporadic cases of MTC.

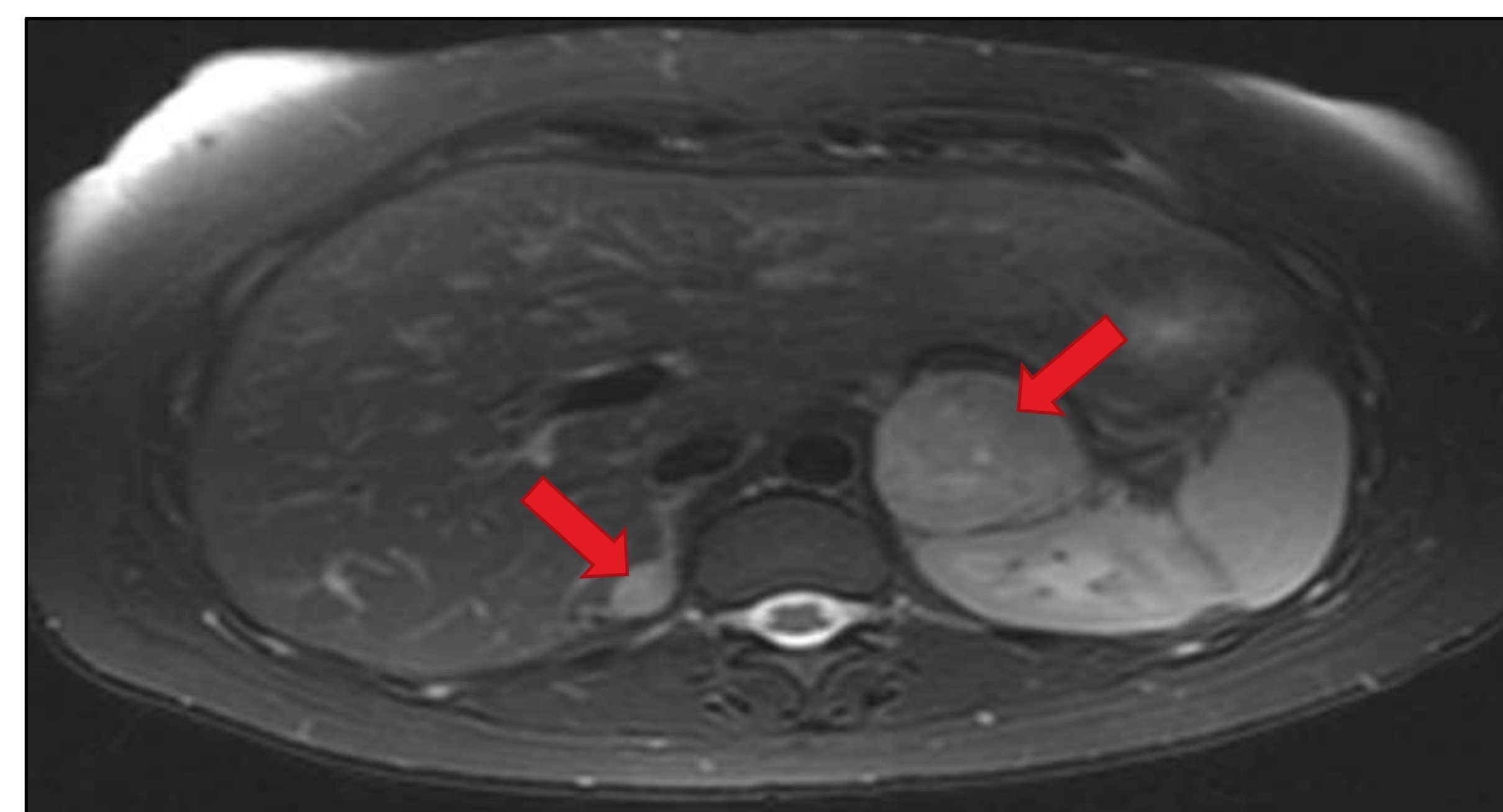


Figure 4-CT Scan of bilateral pheochromocytoma (arrows) in a patient with MTC. Pheochromocytoma is present in approximately 50% of MEN2A and MEN 2B patients.



Figure 5- Eyelid and tongue neuromas and eyelid inversion characteristic of MEN2B.

◆ Conclusion

Although our experience with MTC is small, we found that MTC represents approximately 5% of all thyroid cancers treated at our center. This is in line with the incidence rates seen in the literature. It was difficult through retrospective chart review to determine decision-making algorithms and outcomes. This may be specific to our region, where referrals and care tend to be fragmented. A protocol-based multidisciplinary approach for these patients would ensure that patients receive appropriate treatment and follow-up.

◆ References

- Callender GG, Hu MI, Evans DB, Perrier ND. *Medullary Thyroid Carcinoma*. Endocrine Surgery. Morita SY, Dackiw APB, Zeiger MA. New York: McGraw-Hill Medical, 2010. 89-109
- Callender GG, Rich TA, CGC, Perrier, ND. *Multiple Endocrine Neoplasia Syndromes*. Surg Clin N Am 2008; **88**:863-895
- Kloos RT, Eng C, Evans DB, et al. *Medullary Thyroid Cancer: Management Guidelines of the American Thyroid Association*. Thyroid 2009; **19**:565-607
- Elisei R, Romei C, Cosci B, et al. *RET point mutations in Thyroid Carcinoma*. Atlas Genet Cytogenet Oncol Haematol 2008

◆ Acknowledgements

Many thanks to the Division of Surgical Oncology, University of Louisville Department of Surgery and NCI R25 grant support University of Louisville Cancer Education Program NIH/NCI (R25-CA134283) for making this opportunity possible.

ASSESSING THE HARVARD SCALE OF BREAST COSMESIS: AN ANALYSIS OF PATIENTS TREATED WITH BREAST CONSERVING THERAPY ON A PHASE II CLINICAL TRIAL



Allison M. Hunter, BA and Anthony E. Dragun, MD

Department of Radiation Oncology, James Graham Brown Cancer Center; University of Louisville School of Medicine, Louisville, Kentucky

ABSTRACT

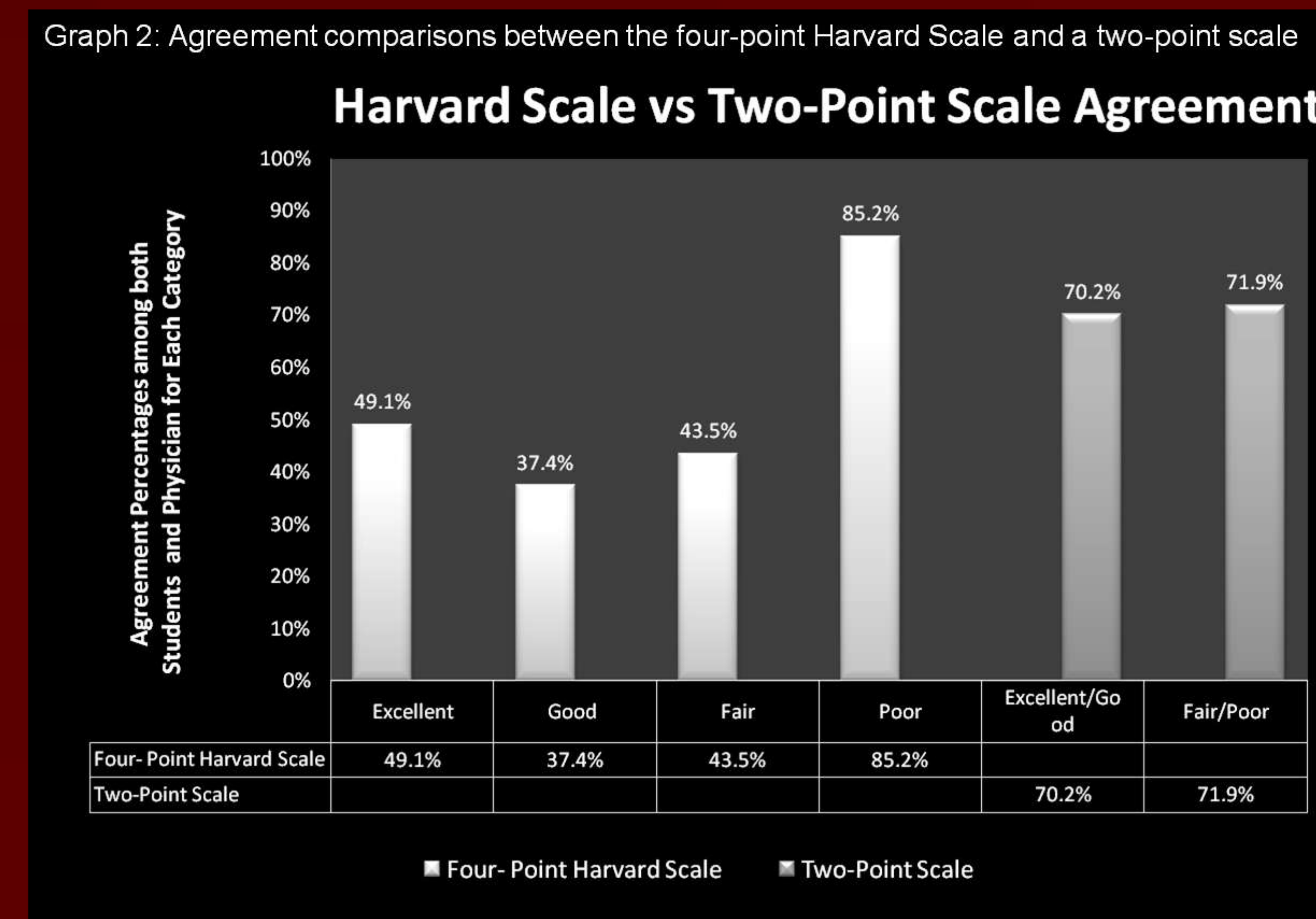
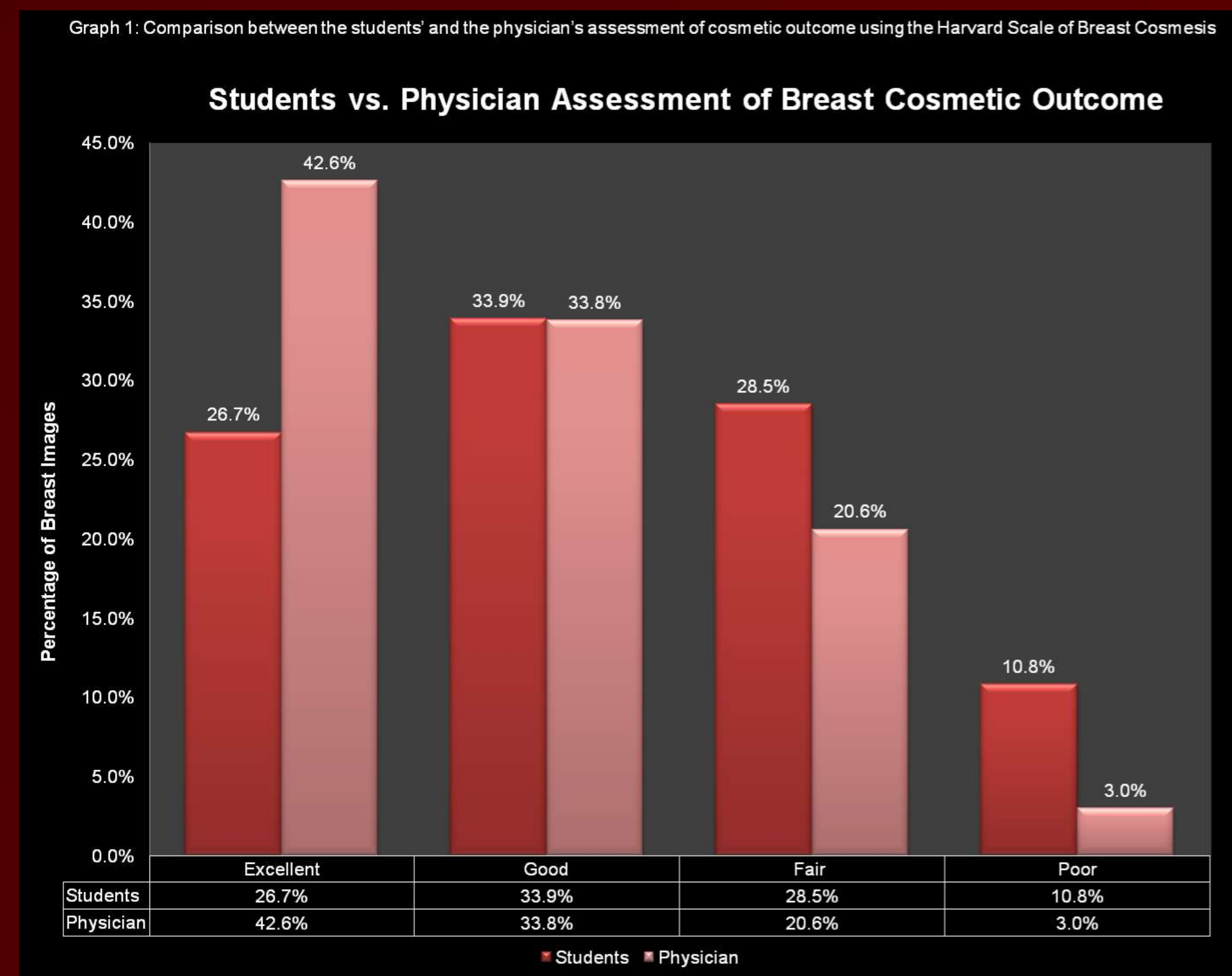
Purpose: Cosmetic outcome is frequently used to assess quality of life (QOL) outcomes in patients that have undergone treatment for breast cancer. As such, an evaluation of the quality and objectivity of the Harvard Scale, a commonly-used assessment tool utilized to evaluate cosmetic outcome in breast cancer patients, is important in gauging objective and congruent QOL expectations following breast cancer treatment.

Materials and Methods: Seventeen (17) patients enrolled on a Phase II protocol, involving Accelerated Hypofractionated Radiotherapy after Breast Conserving Surgery for early stage breast cancer treatment, were assessed at four post-operative time points within a one-year window following radiation treatment. Each time point assessment was completed by the treating physician using the four-tier Harvard Scale (Excellent, Good, Fair, Poor) to compare the treated breast to the controlled breast. A survey including the same de-identified images was then distributed to forty-four (44) medical students and residents in hopes of assessing the validity of the Harvard Scale.

Results: Of the 44 medical student and resident respondents, there was equal distribution between male (23) and female (21), with the majority of respondents describing themselves as single (82%), Caucasian (70%), and less than twenty-nine (29) years of age (89%). The physician's assessment of cosmetic outcome differed somewhat from the respondent averages: Excellent (43% vs. 27%), Good (34% vs. 34%), Fair (20% vs. 28%) and Poor (3% vs. 11%). Congruence between the physician and the respondents in the same four categories showed to be 49%, 37%, 44%, and 86%, respectively. Finally, when combining the categories into a bimodal representation of Excellent/Good (70%) versus Fair/Poor (72%), there was a significant increase in congruence between the treating physician and the respondents.

Conclusion: Evaluation of cosmetic outcome following treatment for early stage breast cancer can be a subjective process, often differing from evaluator to evaluator. Our results suggest that a two point scale in place of the four-point Harvard Scale would be a better method to evaluate cosmetic outcome due to the significant improvement in congruity among evaluators.

DATA ANALYSIS GRAPHS



THE HARVAD SCALE OF BREAST COSMESIS

PLEASE ASSESS BREAST COSMESIS AT THIS TIME. (Circle the number next to the word that best describes the cosmetic results.)

1	EXCELLENT: when compared to the untreated breast or the original appearance of the breast, there is minimal or no difference in the size or shape of the treated breast. The way the breast feels (its texture) is the same or slightly different. There may be thickening, scar tissue or fluid accumulation within the breast, but not enough to change the appearance.
2	GOOD: there is a slight difference in the size or shape of the treated breast as compared to the opposite breast or the original appearance of the treated breast. There may be some mild reddening or darkening of the breast. The thickening or scar tissue within the breast causes only a mild change in the shape or size.
3	FAIR: Obvious differences in the size and shape of the treated breast. This change a quarter or less of the breast. There can be moderate thickening or scar tissue of the skin and the breast, and there may be obvious color changes.
4	POOR: marked change in the appearance of the treated breast involving more than a quarter of the breast tissue. The skin changes may be obvious and detract from the appearance of the breast. Severe scarring and thickening of the breast, which clearly alters the appearance of the breast, may be found.

DEMOGRAPHIC INFORMATION

Table 1: Demographic comparison of survey participants

Demographic Variables	Frequency	Percentage
Gender		
Male	23	52.2%
Female	21	47.7%
Age Range		
21-29 years	39	88.6%
30-39 years	5	11.3%
Ethnicity		
Caucasian	31	70.4%
African-American	4	9.0%
Asian	4	9.0%
East Indian	3	6.8%
Middle Eastern	2	4.5%
Hometown Location		
Suburban	31	70.4%
Urban	6	13.6%
Rural	7	15.9%
Level of Education		
Medical Student	34	77.3%
Resident	10	22.7%
Ideal Type of Medical Practice		
Academics	23	52.2%
Private Practice	15	34.0%
Other	6	13.6%



Contact Information:

Allison M. Hunter

University of Louisville School of Medicine

amhunt01@louisville.edu

University of Louisville Cancer Education

Program Participant

NIH/NCI R25 grant support

Identifying urine exosome miRNA profiles in melanoma patients

Daniel J. Kmetz, B.S.¹, Deyi Xiao, M.D. ¹, Michael Egger, M.D. ¹, Sabine Waigel, M.S. ², Wolfgang Zacharias, Ph.D. ², Hongying Hao, M.D., Ph.D.¹, Kelly M. McMasters, M. D., Ph. D.¹,
Departments of Surgery¹, University of Louisville School of Medicine
Microarray Facility², University of Louisville School of Medicine

Abstract

Background: Melanoma is a highly heterogeneous malignant tumor with a wide range of prognoses among stages based on the American Joint Committee on Cancer (AJCC) groupings. A need exists for developing biomarkers that can aid in melanoma diagnosis, prognosis, and follow-up. Exosomes are 40-100nm diameter membrane vesicles released from tumors into the body fluids such as urine. Unique miRNA in tumor exosomes contributes to malignant progression through post-translational silencing of mRNA. This leads to the possibility of characterizing differences in expression of exosomal miRNA of melanoma and non-melanoma patients in the search for a biomarker for assessment of the disease process.

Materials and Methods: This study used urine collected from non-melanoma, Stage I, and Stage IV melanoma patients to isolate exosomes. Western blot and electron microscopy were used to assess purity of exosome. Urine exosome RNA were isolated and applied to Affymetrix miRNA array 2.0. Differentially expressed miRNAs across the three sample groups were analyzed by ANOVA.

Results: The results showed that stage I melanoma patients had 10% greater yield of exosome RNA than that of our control group, and Stage IV patients had 20% higher yield of RNA than that of Stage I patients. 33 differentially expressed miRNAs were found in Stage I vs Control group. Among them were miR-3201, miR-3128, miR-3148, miR-378, miR-320a, and miR-320b. 17 differentially expressed miRNAs were identified in Stage IV vs control group, such as miR-548a-3p, miR-103, miR-30c, miR-93, and miR-191.In comparison of Stage IV vs Stage I melanoma patients, there were 5 miRNAs (miR-1825, miR-1972, miR-1184, miR-3201, and miR-940) with significant changes. There were 9 significant expressed miRNAs detected in both Stage I vs Control and Stage IV vs Control groups. A database search of these miRNAs' function revealed some of the miRNAs have been previously implicated in cancer process, but many have no known function.

Conclusion: To our knowledge this is the first attempt to analyze urine exosomal RNA profiles in melanoma patients. These distinctive urine exosomal miRNA signatures may be used as diagnostic and prognostic markers for melanoma patients. This research could lead to translation into a non-invasive method for identifying diagnostic and prognostic biomarkers in melanoma patients.

Introduction

- Exosomes** are 40-100nm membrane bound vesicles excreted in excess from tumor cells into body fluids such as urine.
- Exosomal microRNA (miRNA)** have recently been shown to play a role in malignant progression.
- miRNA** is small, noncoding RNA that posttranscriptionally silences mRNA.
- Analyzing exosomal miRNA signatures in melanoma patients could identify a potential noninvasive biomarker.

Methods

Patient Groups:

- Non-melanoma
 - Stage I Melanoma
 - Stage IV Melanoma
- Exosomes were isolated from urine using a modified ExoQuick-TC protocol. Western blot and electron microscopy were used to assess purity of exosome.
 - RNA was isolated from exosome and miRNA array was conducted using Affymetrix miRNA array 2.0.
 - Differentially expressed miRNAs across the three sample groups were analyzed by ANOVA.

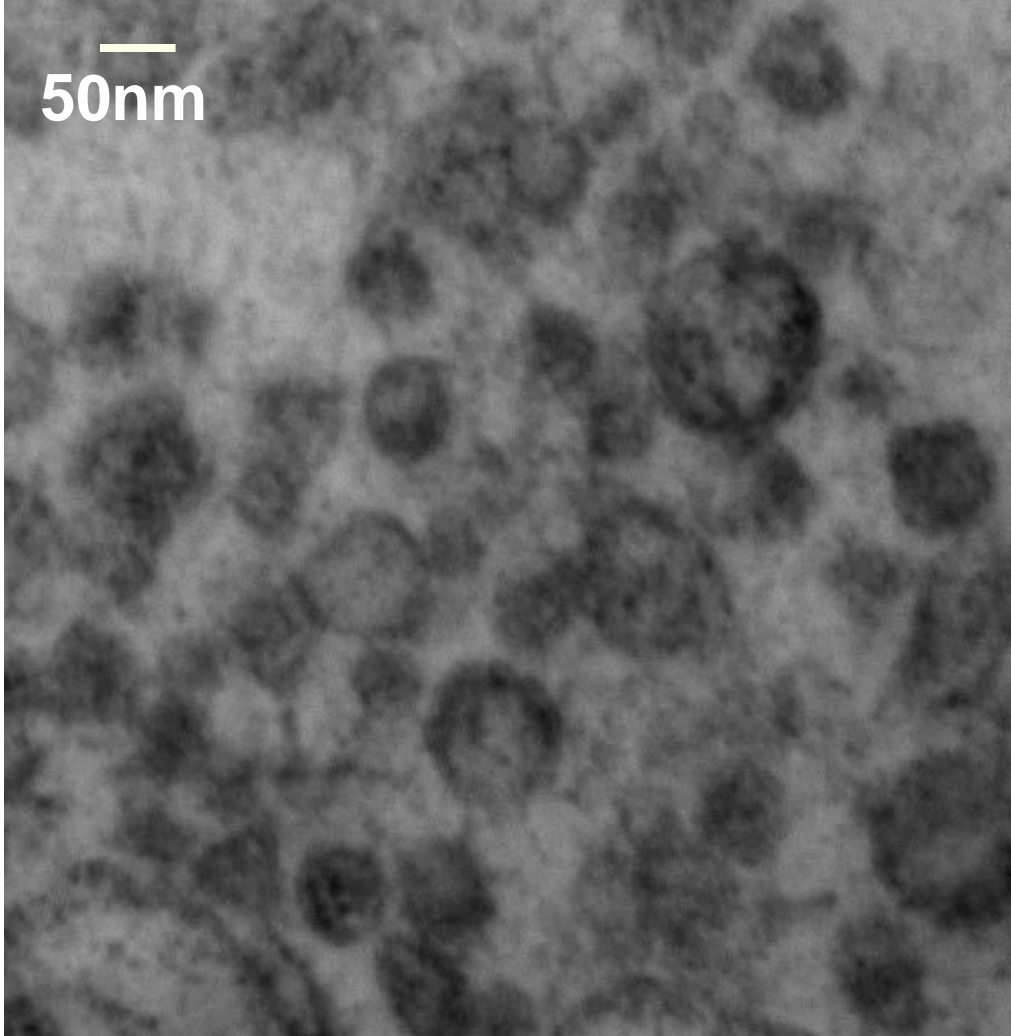


Figure 1. Electronic microscope confirmed the purity of exosomes.

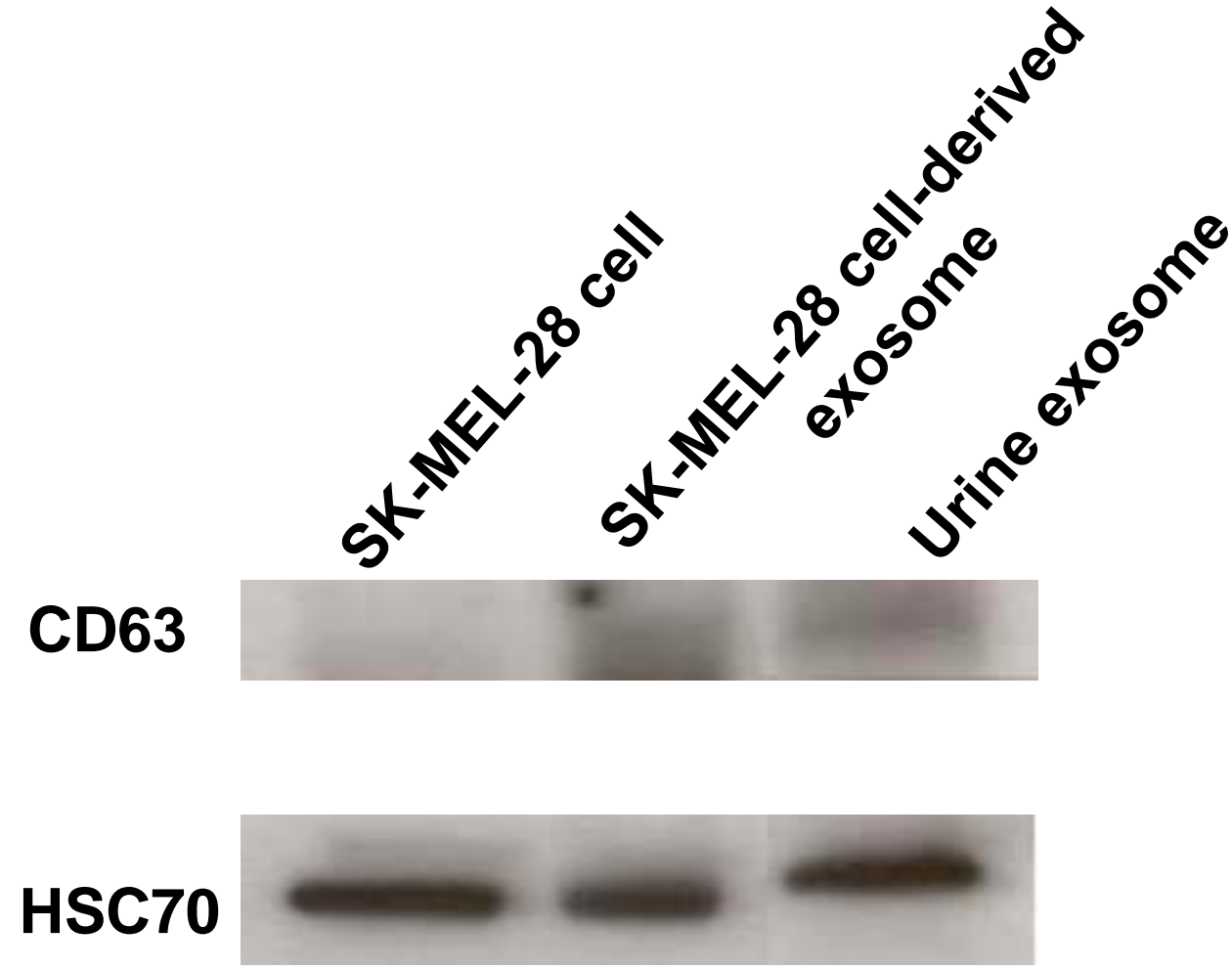


Figure 2. Western blot of urine exosome.

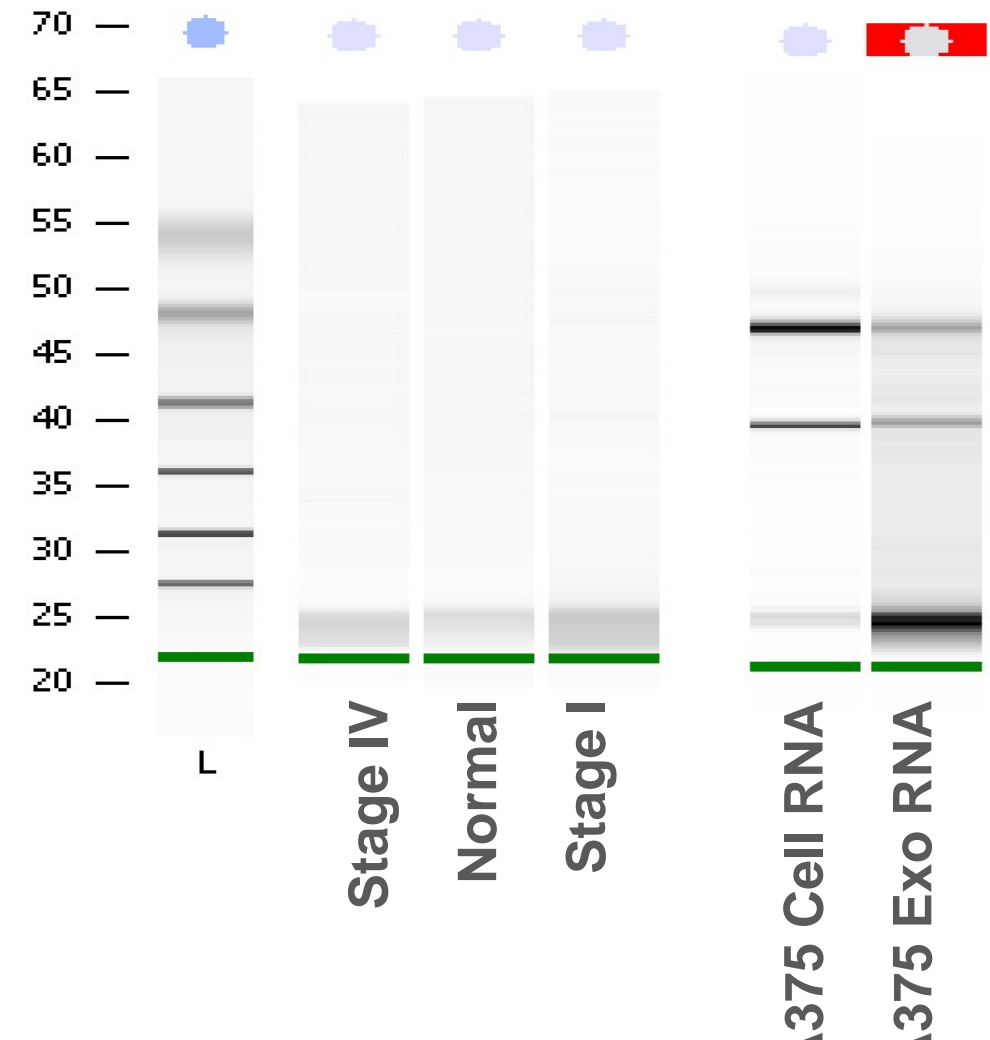


Figure 4. Bioanalyzer results reveal exosome RNA quality.

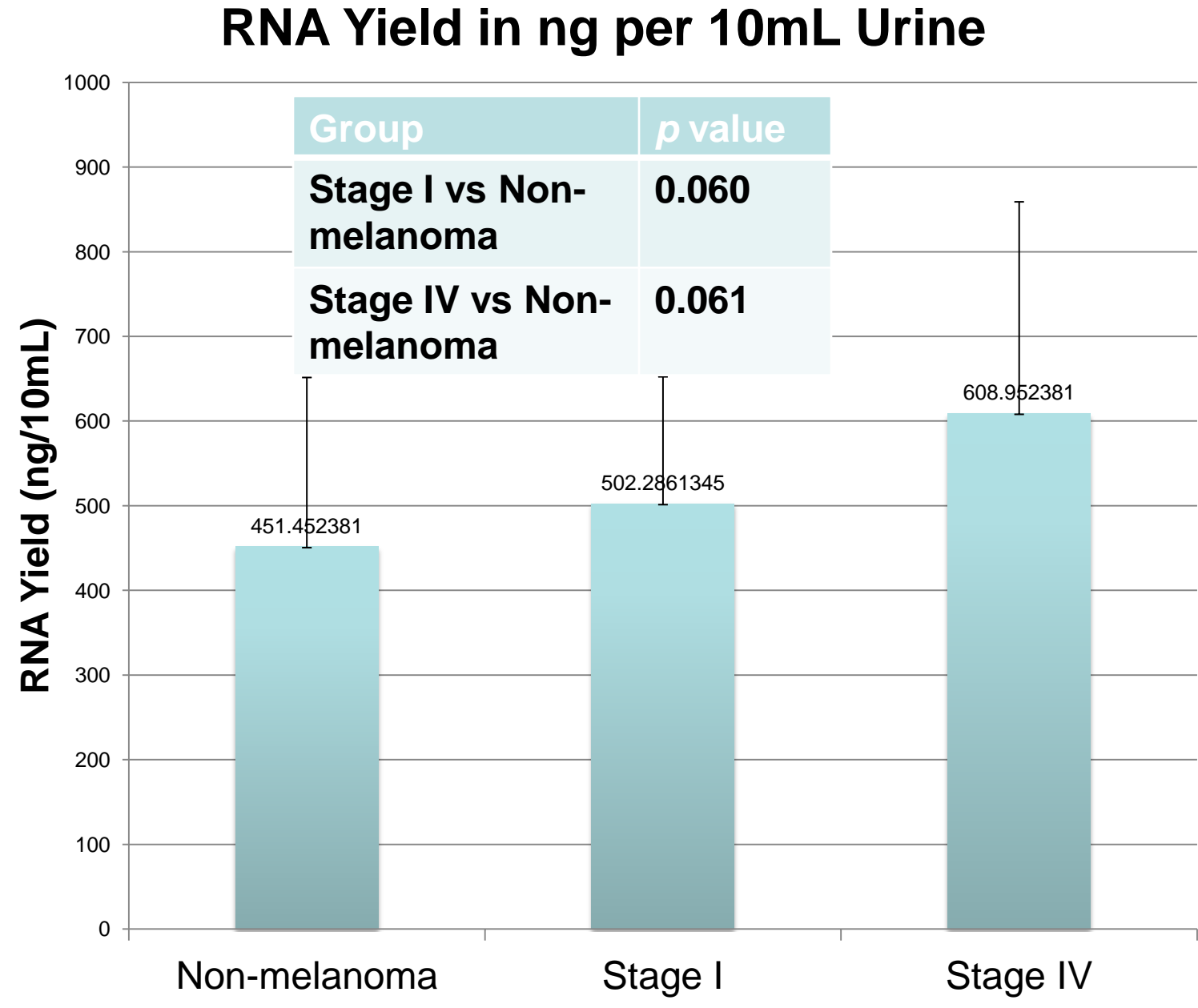


Figure 5. Average RNA yield per 10mL of urine for each sample group.

Results

Table 2. Differential expressed miRNAs (stage I vs. non-melanoma) ($P<0.05$, $-2>FC>2$) (4 shown of 33 found)

miRNA	Fold Change	p value	Implicated in
hsa_mir_320c	-4.63	.00456	Apoptosis, proliferation, migration of various cancers
hsa_mir_205	-4.60	.0129	Apoptosis, migration in MM and other cancers
hsa_mir_378	-4.35	.0287	Growth in various cancers
hsa_mir_320a	-4.28	.0109	Altered expression in various cancers

Table 3. Differential expressed miRNAs (stage IV vs. non-melanoma) ($P<0.05$, $-2>FC>2$) (4 shown of 17 found)

miRNA	Fold change	p value	Known role
Hsa_mir_100	-2.11	.0205	Cell viability and proliferation in melanoma and other cancers
Hsa_mir_103	-	-	-
Hsa_mir_30c	-3.45	.0412	Transcription and differentiation in various cancers
Hsa_mir_93	-3.16	.0373	Cell cycle, proliferation and chemotherapy resistance in various cancers

Table 4. Differential expressed miRNAs (stage IV vs. stage I) ($p<0.05$, $FC >2 <-2$) (2 shown of 5 found)

miRNA	Fold Change	p value	Role
hsa_mir_1825	-2.1	.0106	Invasion and metastasis of various cancers
hsa_mir_1972	-2.32	.00277	Proliferation in various cancers

Table 5. Overlapped differential expressed miRNAs (stage I vs. non-tumor and stage IV vs. non-tumor) ($p<0.05$, $-2>FC>2$) (5 shown of 9 found)

miRNA	p-value (Stage I vs non-mela.)	Fold-Change (Stage I vs non-mela.)	p-value (Stage IV vs non-mela.)	Fold-Change (Stage IV vs non-mela.)
hsa-let-7i	0.00291099	-2.61841	0.0205333	-2.11152
hsa-miR-100	0.00305561	-2.19087	0.0105549	-2.14701
hsa-miR-103	0.00334644	6.03427	0.0426329	-2.24698
hsa-miR-106b	0.00525224	-2.53161	0.0219002	-2.52945
hsa-miR-502-3p	0.0392121	-2.62913	0.0373013	-3.16274

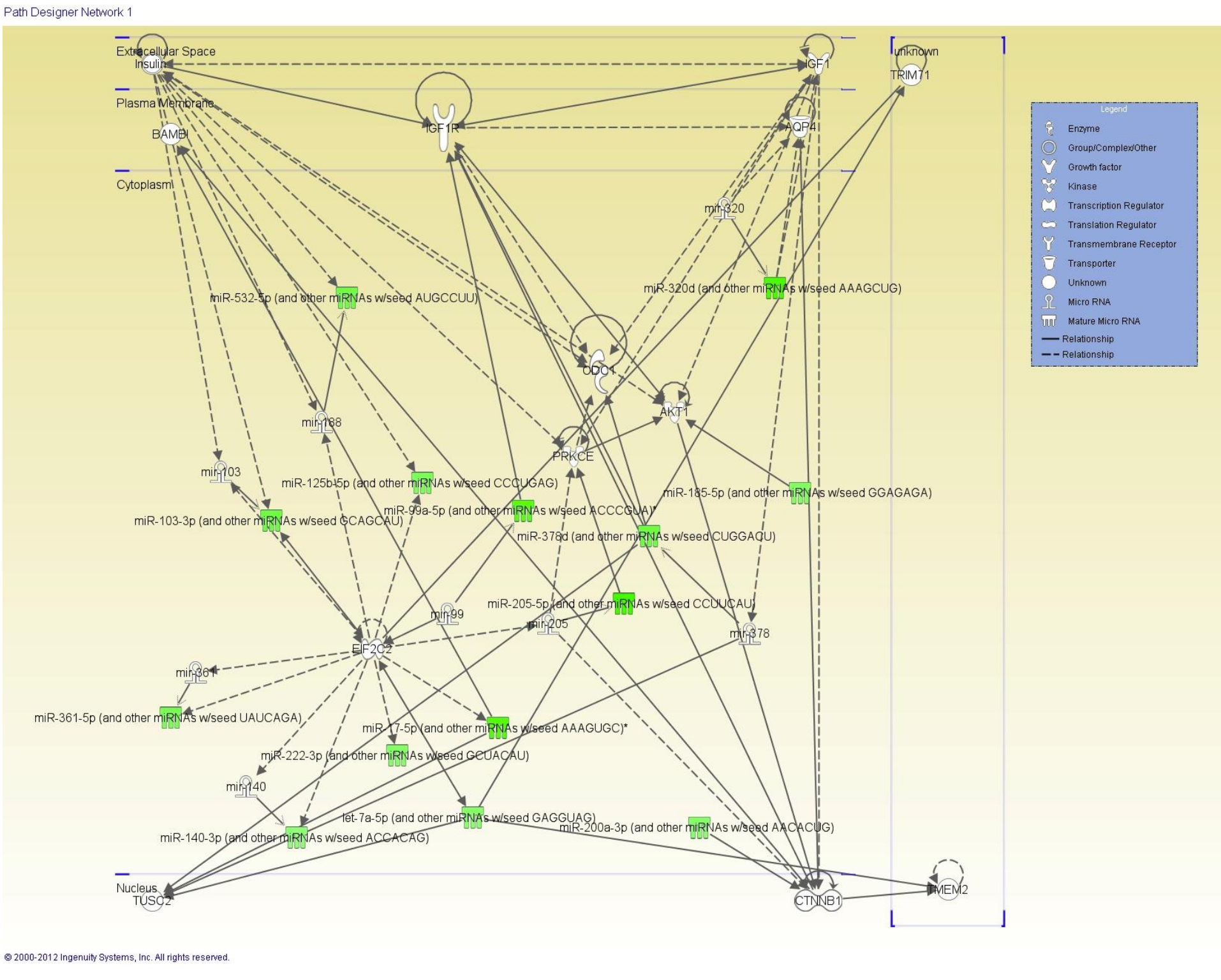


Figure 6. Cancer related differentially expressed miRNAs in Stage I vs non-melanoma. Green=downregulated

Conclusions

- Larger amounts of urine exosomes were found in melanoma patients than those in non-tumor patients.
- There are specific exosomal miRNAs found in Stage I and IV melanoma patients compared to non-melanoma patients.
- While some of these specific miRNAs have been previously associated with malignant tumors, most have no known function and could be specific melanoma markers.
- These results provide a starting point for identifying a miRNA signature of melanoma-derived exosomes. The clinical translation into a non-invasive diagnostic and prognostic biomarker is a real possibility.

Acknowledgements

Research supported by NCI R25 grant University of Louisville Cancer Education Program NIH/NCI (R25-CA134283), grant from Melanoma Research Foundation, and University of Louisville Clinical & Translational Science Pilot Grant Innovative Award to K.M.M.

Translocase Activity in Parotid Acinar Cells

McKinley Soult¹, Venkatesh Srirangapatnam, Ph.D¹, Anne L. Carenbauer¹, Douglas Darling, Ph.D.^{1,2}

¹Dept. of Oral Health and Rehabilitation, ²Dept. of Biochemistry & Molecular Biology University of Louisville School of Dentistry

Introduction

Salivary glands have a critical role in maintaining the dynamic equilibrium of the oral cavity. Saliva has antimicrobial properties, lubricates food for swallowing and initiates carbohydrate digestion. Salivary gland cancers occur in approximately one in every 50,000 people each year in the United States. Recent studies suggest that translocases (adenine nucleotide translocase²) or flippases /floppases (P-glycoprotein¹; MDR1¹; ABCB1¹) are factors in eliciting cancer cell death and promising therapeutic targets. Additionally, lipid flippases/floppases or scramblases may play a role in sorting of salivary secretory proteins in the parotid gland. Our objective was to identify which flippases are present in the parotid gland and determine their location in the acinar cell.

Methods

The presence of translocases or flippases/floppases was determined by PCR and immunocytochemistry. Total RNA was isolated from the parotid glands of healthy adult Sprague-Dawley rats and quantiated. cDNA from the total RNA was synthesized using the High Capacity cDNA Reverse Transcriptase Kit (Applied Biosystems) following the manufacturer's protocol. The cDNA was then used for analytical and quantitative PCR. Primers for specific flippases/floppases or translocases were designed from mRNA sequences selected from NCBI nucleotide databases. The analytical PCR products were visualized by agarose gel (1%) electrophoresis. The mRNA levels for the selected proteins were quantitated by real-time PCR using the QuantiTect SYBR Green kit protocol and the expression normalized to GAPDH. A select few proteins were localized by immunofluorescence on paraffin-embedded adult parotid tissue sections. Prior to immunohistochemistry (IHC), the parotid sections were subjected to antigen retrieval. The tissue was then blocked with 10% normal goat serum in phosphate buffer saline, pH 7.3, (PBS) and incubated overnight with primary antibodies either to ABCA1 or ABCG1. Following washes with PBS, the section was incubated with FITC-tagged anti-rabbit IgG, washed and the binding visualized on an Olympus FV500 confocal microscope.

Results

Figure 2a

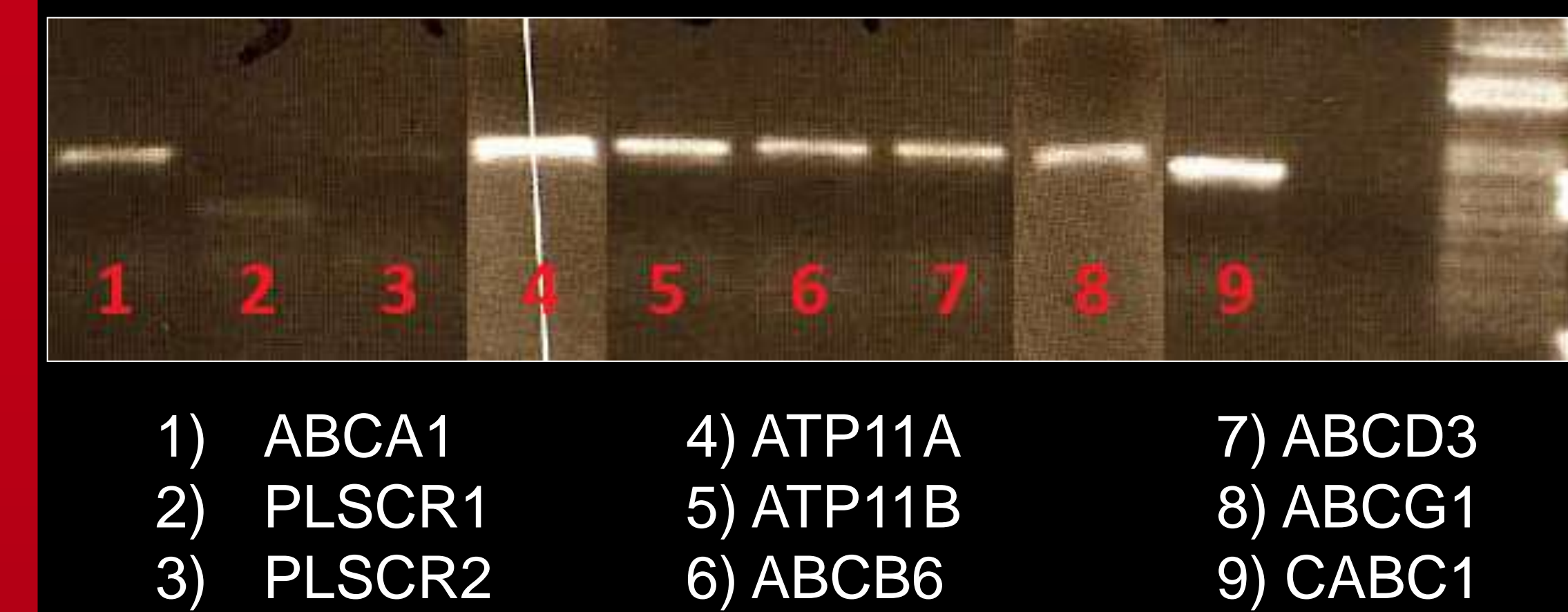
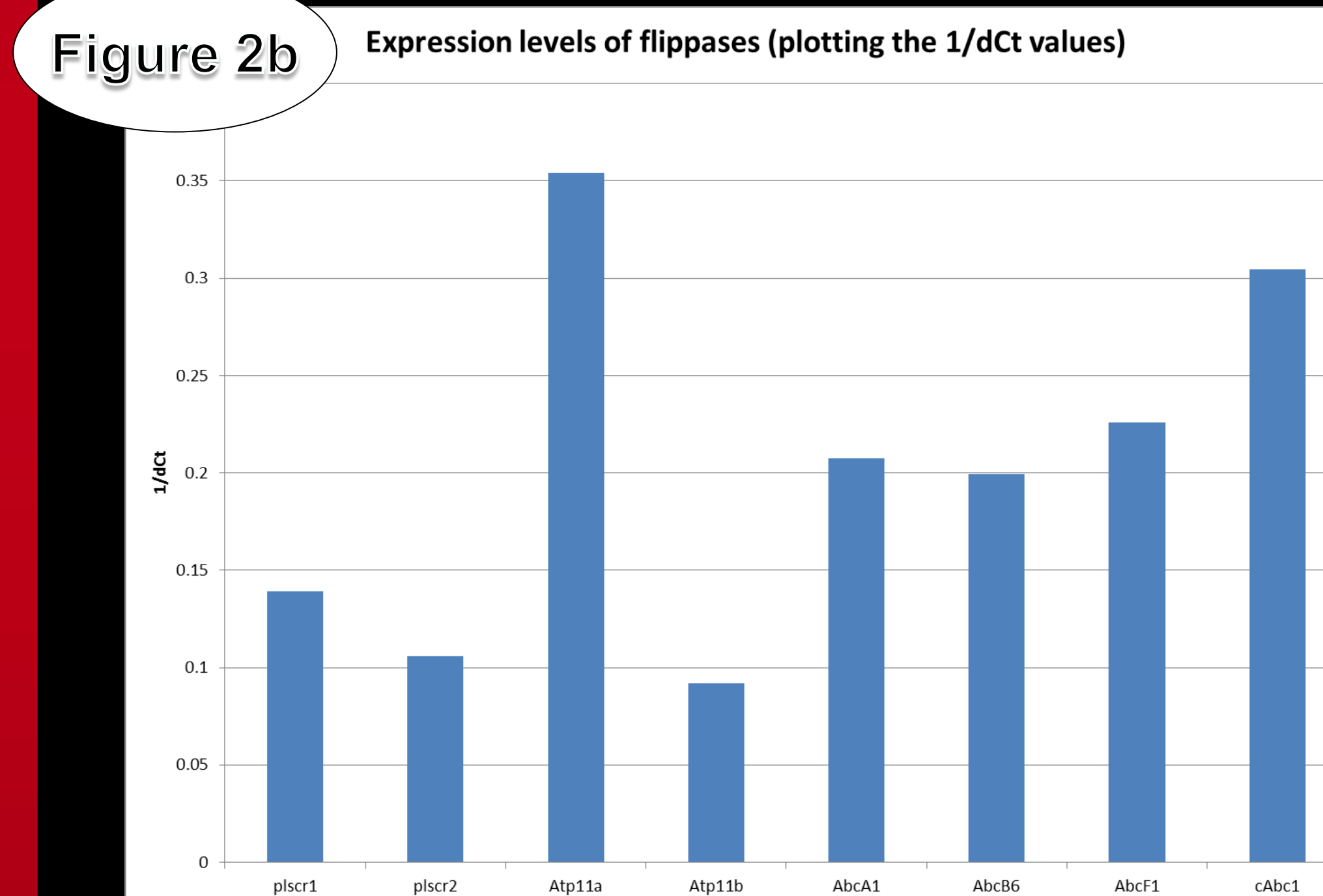
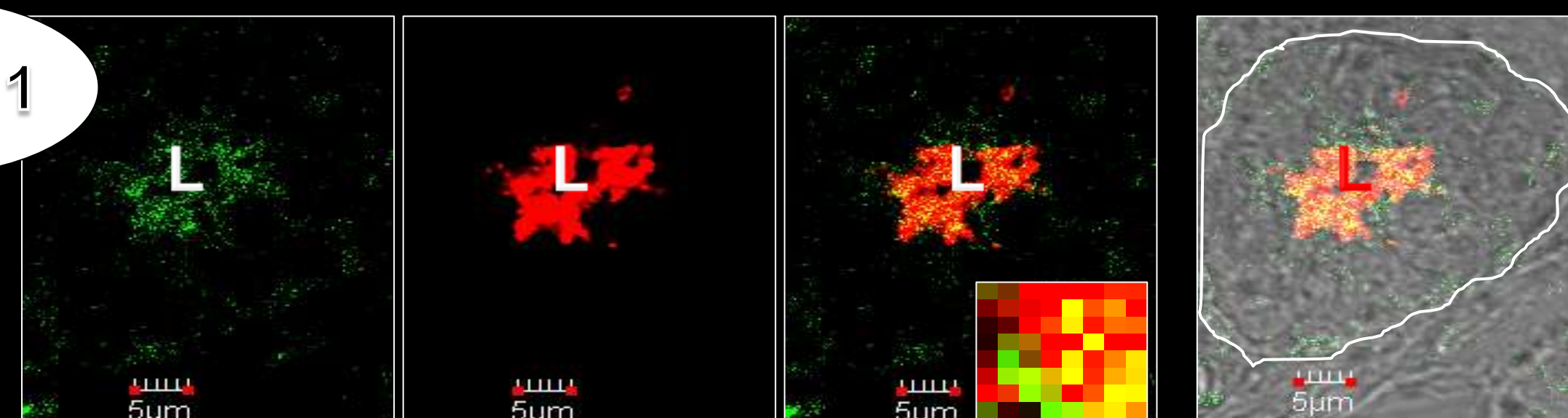


Figure 2b



2a) PCR products of mRNA primers. ATP11A (4) and CABG1 (9) showed strong bands while PLSCR1 (2) PLSCR2 (3) expressed weak bands. ABCA1 (1), ATP11B (5), ABCB6 (6), ABCD3 (7) and ABCG1 (8) expressed moderate bands. All primers showed no product in negative reverse transcriptase controls. 2b) RT-PCR analysis confirmed results of PCR. Individual threshold values were subtracted from the control GAPDH threshold. Reciprocal values were then calculated and plotted.

Figure 1



Co-localization of PSP and PI3,4P₂ lipid towards the lumen (L) in parotid acinar cells.

Figure 3a

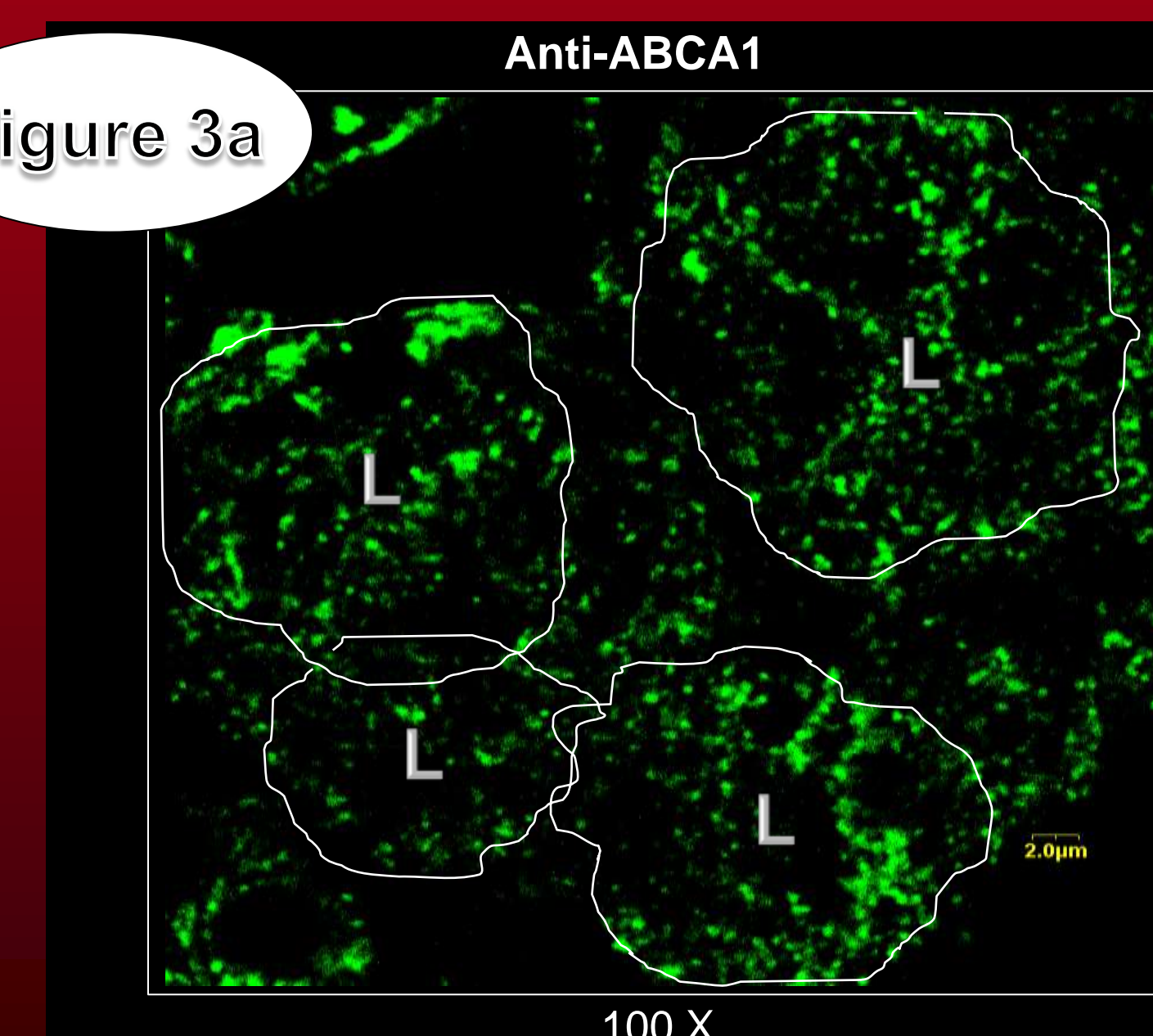


Figure 3b

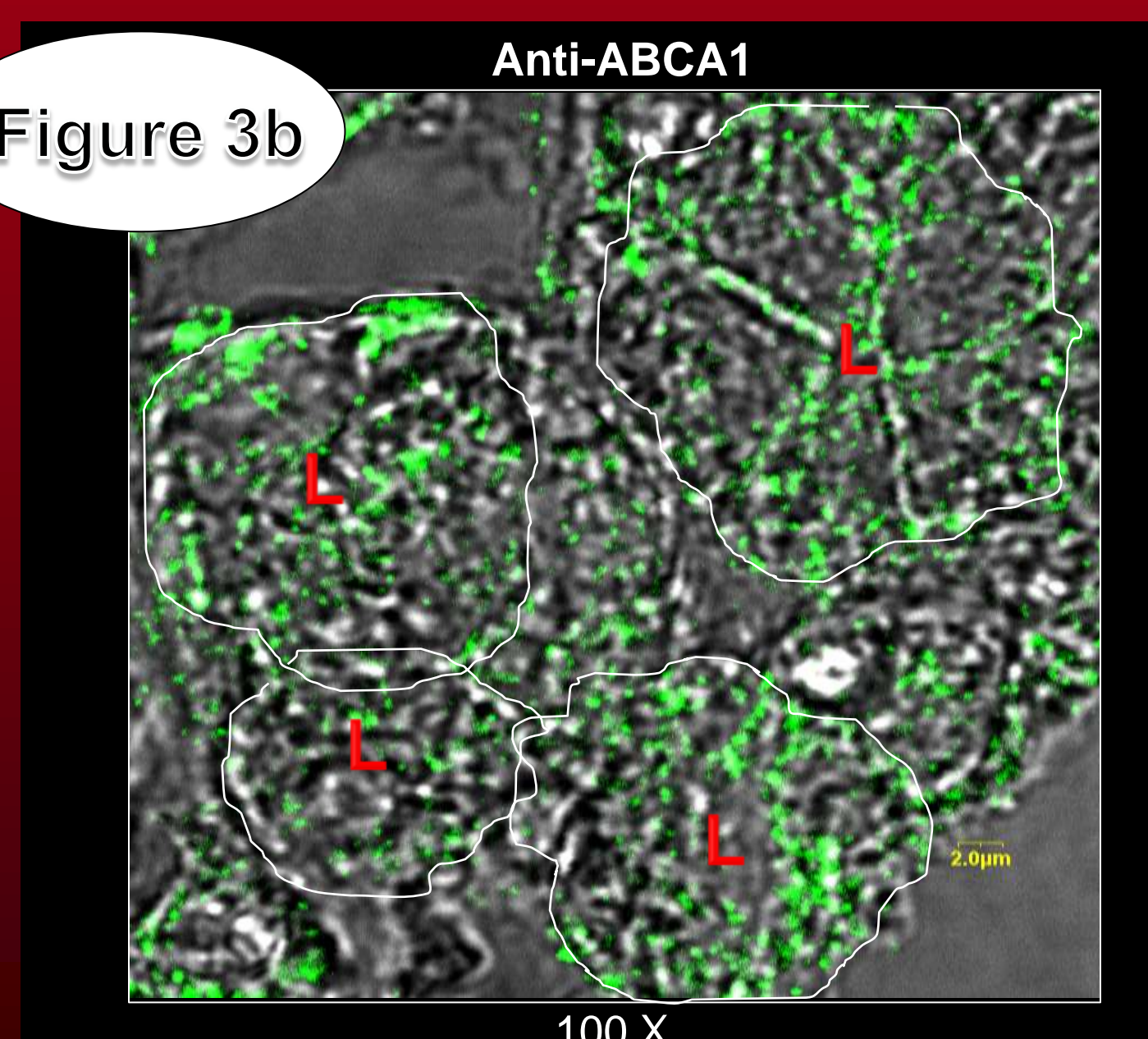
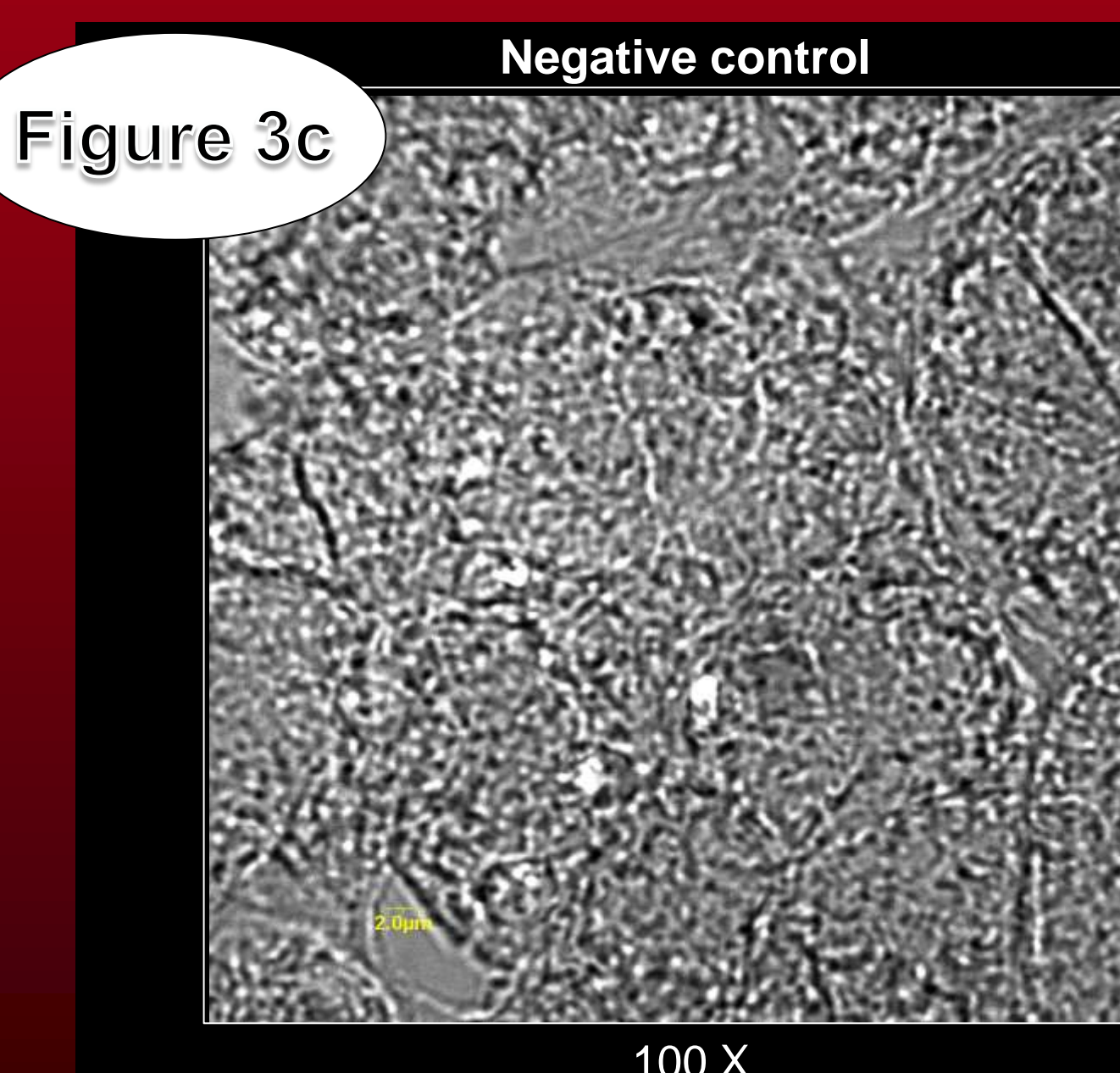


Figure 3c



Immunocytochemistry was performed on adult rat parotid gland paraffin sections to determine the pattern of expression of ABCA1 and ABCG1. Parotid sections were labeled with anti-ABCG1 or anti-ABCA1. The anti-ABCG1 antibody showed no specific immunoreactivity. 3a) Anti-ABCA1 in parotid acinar cells localized on apical and basolateral membranes and potentially secretory granules, (L denotes lumen of acinus), 3b) differential interference contrast microscopy over laid upon image 3a to reinforce acinar structure, 3c) DICM image of parotid acini.

Previous microarray analyses in the lab suggested the presence of the flippases/floppases ABCA1, ABCB6, ABCD3, ABCF1, ABCG1, ATP11A, ATP11B, CABG1 and the scramblases PLSCR1 and PLSCR2, during parotid gland development. In the present investigation PCR analysis of these proteins demonstrated strong bands for ATP11A and CABG1 genes and weak bands for PLSCR1 and PLSCR2 genes. Quantitative PCR analysis showed a high level of expression for ATP11A suggesting that it could be the major flippase of the parotid gland, followed by CABG1. ABCA1, ABCB6 and ABCF1 were also strongly expressed. ATP11B, ABCG1, PLSCR1 and PLSCR2 were weakly expressed. Immunocytochemistry revealed strong localization of ABCA1 at apical and basolateral cell membranes and potentially in secretory vesicles. ABCG1 was not detected.

Discussion

It is important to understand acinar cell differentiation and secretory mechanisms to reactivate or regenerate the cell systems and tissue, respectively, in patients with loss of salivary gland function. IHC revealed localization of the cell membrane lipid translocation protein ABCA1 near apical and basolateral parotid acinar cell membranes and potentially secretory vesicles. ABCA1 could be involved in parotid acinar cholesterol transport since its primary mechanism throughout the body is cholesterol transport. ABCG1 did not localize. ATP11A and CABG1 had the highest mRNA expression and should be examined under IHC.

Conclusions

Several flippases/floppases or scramblases that could be potentially involved in the secretory process are found in the healthy parotid gland. ATP11A and CABG1 had the highest levels of mRNA expression of those studied. IHC revealed localization of ABCA1 in the cell membrane and possibly in secretory granule membranes. Further analysis of these proteins will help elicit their role in protein sorting in the parotid gland.

Acknowledgements

Research supported by a grant by the National Cancer Institute grant R25-CA134283.

References

- Dean, M., Andrey, R., Allikmets, R. The Human ATP-Binding Cassette (ABC) Transporter Superfamily *Genome Res* 2001 11:1156–1166
- Le Bras, M., Borgne-Sanchez, A., Touat, Z., et al. Experimental Therapeutics, Molecular Targets and Chemical Biology; Chemosensitization by Knockdown of Adenine Nucleotide Translocase-2 *Cancer Res* September 15, 2006 66:9143-9152; doi: 10.1158/0008-5472.CAN-05-4407
- Venkatesh, S.G., Goyal, D., Carenbauer, A.L., Darling, D.S. Parotid Secretory Protein Binds Phosphatidylinositol (3,4) Bisphosphate *J DENT RES* September 2011 90: 1085-1090

HYPOTHESIS

Translocases or flippases/floppases are present in secretory granules in parotid acinar cells.

CaMKII represses CaMKIV transcription to promote proliferation in myeloid leukemia cells

Lauren Strait¹, Cuibo Yang³, Maddalena Illario⁵ and Uma Sankar^{1, 2, 3, 4}

University of Louisville School of Medicine¹; Owensboro Cancer Research Program²

and James Graham Brown Cancer Center³; Department of Pharmacology and Toxicology⁴, University of Louisville and Dipartimento Biologia e Patologia Cellulare e Molecolare, Federico II University⁵

INTRODUCTION

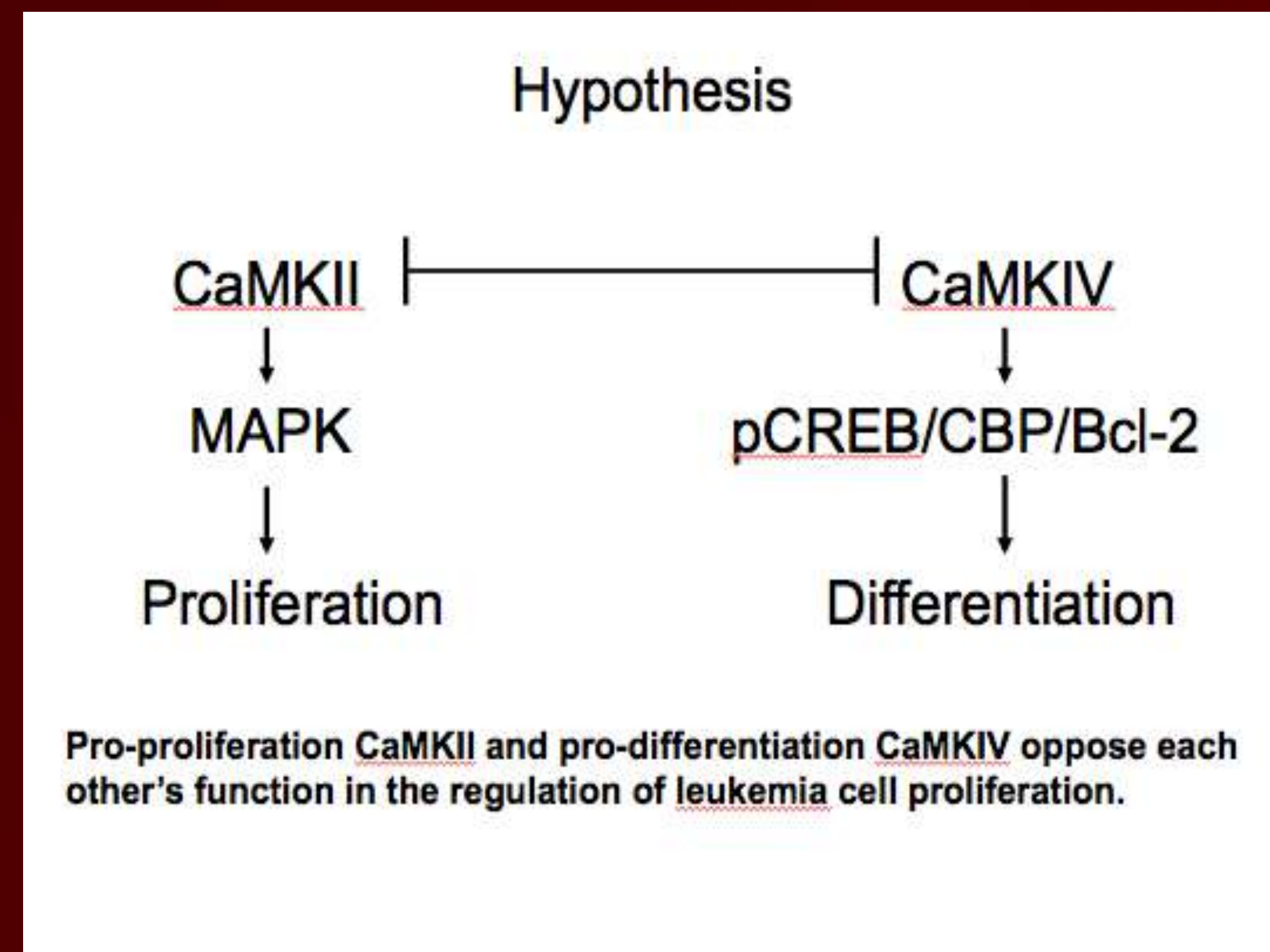
Calcium/Calmodulin dependent protein kinases (CaMK) play an important role in cell signaling cascades by linking increases in intracellular calcium with biological processes. In myeloid leukemia cells, calmodulin dependent protein kinase II (CaMKII) promotes cell proliferation by binding to RAS/RAF and stabilizing the mitogen-activated protein kinase (MAPK) pathway. CaMKII also binds to and phosphorylates retinoic acid receptor (RAR), a nuclear hormone receptor transcription factor. This phosphorylation of RAR increases its interaction with co-repressors causing an inhibition of RAR-mediated gene transcription. Alternatively, CaMKIV is expressed at very low levels in myeloid leukemia cells. However, pharmacological inhibition of CaMKII enhances CaMKIV mRNA and protein expression, potentially through the de-repression of *CaMK4* transcription. The *CaMK4* promoter contains RAR response element (RRE) that can be activated by retinoic acid. Since CaMKII can inhibit RAR-mediated transcription, we hypothesize that increased CaMKII can repress CaMKIV transcription. In this study, we investigated the potential cross talk between CaMKII and CaMKIV in multiple myeloid leukemia cell lines.

REFERENCE

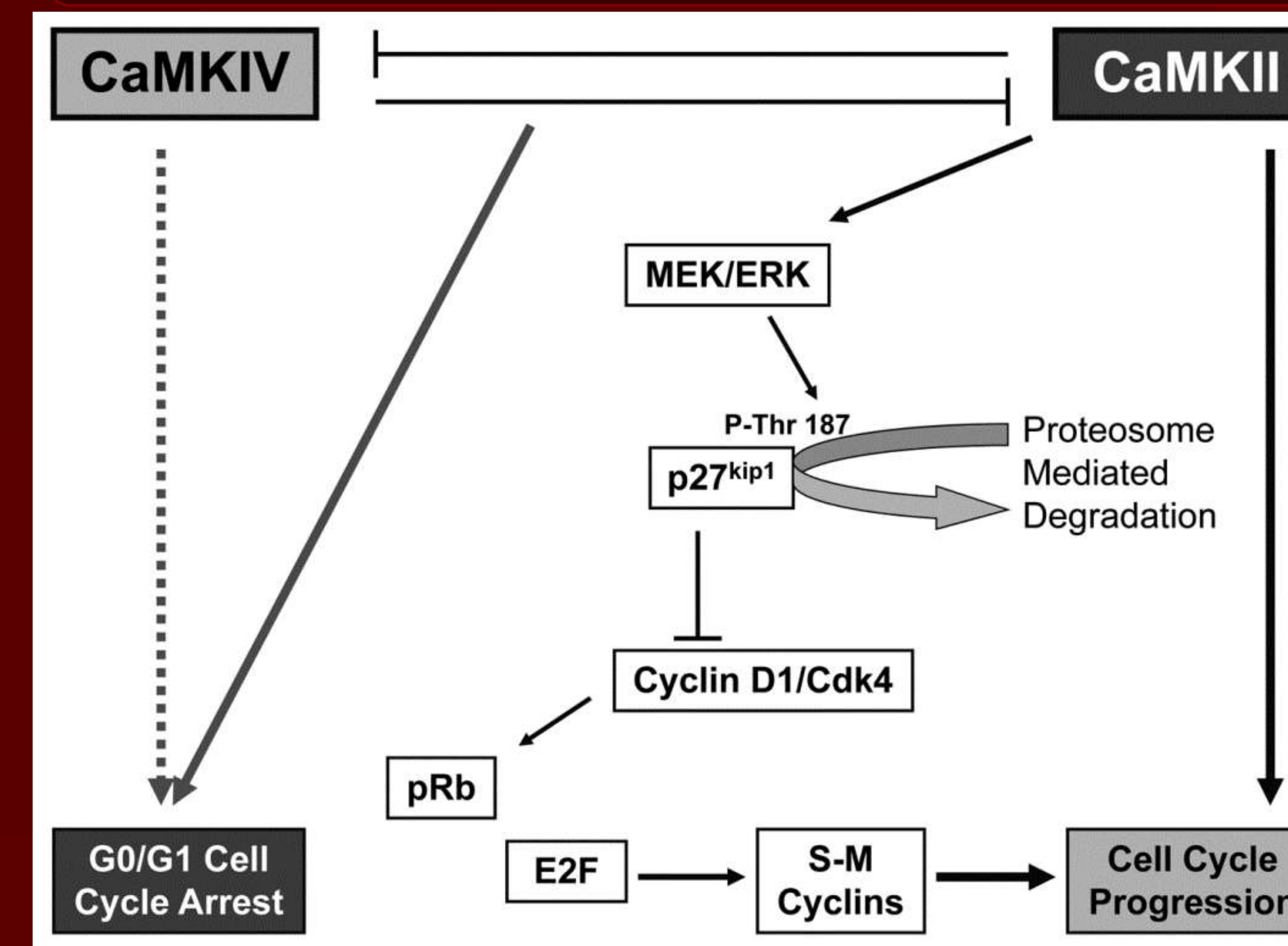
Hook SS, Means AR (2001) Ca(2+)/CaM-dependent kinases: from activation to function. Annu Rev Pharmacol Toxicol 41: 471-505.

Sankar U, Kitsos CM, Illario M, Colomer-Font JM, Duncan AW, et al. (2005) Calmodulin-dependent protein kinase IV regulates hematopoietic stem cell maintenance. J Biol Chem 280: 33101-33108

HYPOTHESIS



MECHANISM



RESULTS

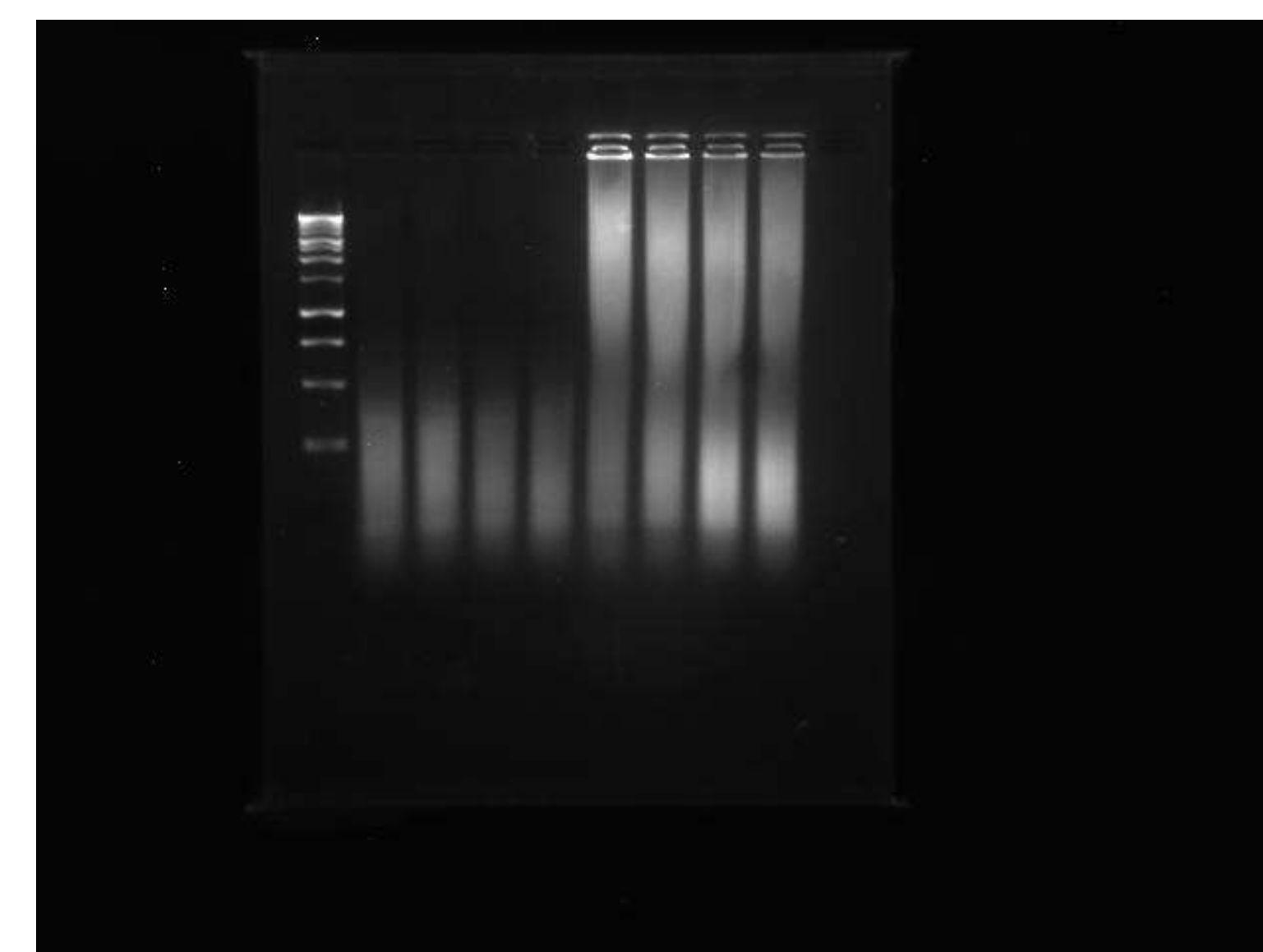


Figure 1: Time course for K562 cells sonicated for 5, 10, 15, and 20 minutes. Wells 1, 2, 3, and 4 contain sonicated chromatin after purification. Wells 5, 6, 7, and 8 contain sonicated chromatin before purification. The optimal fragment size of K562 cells is observed at 10 minutes.

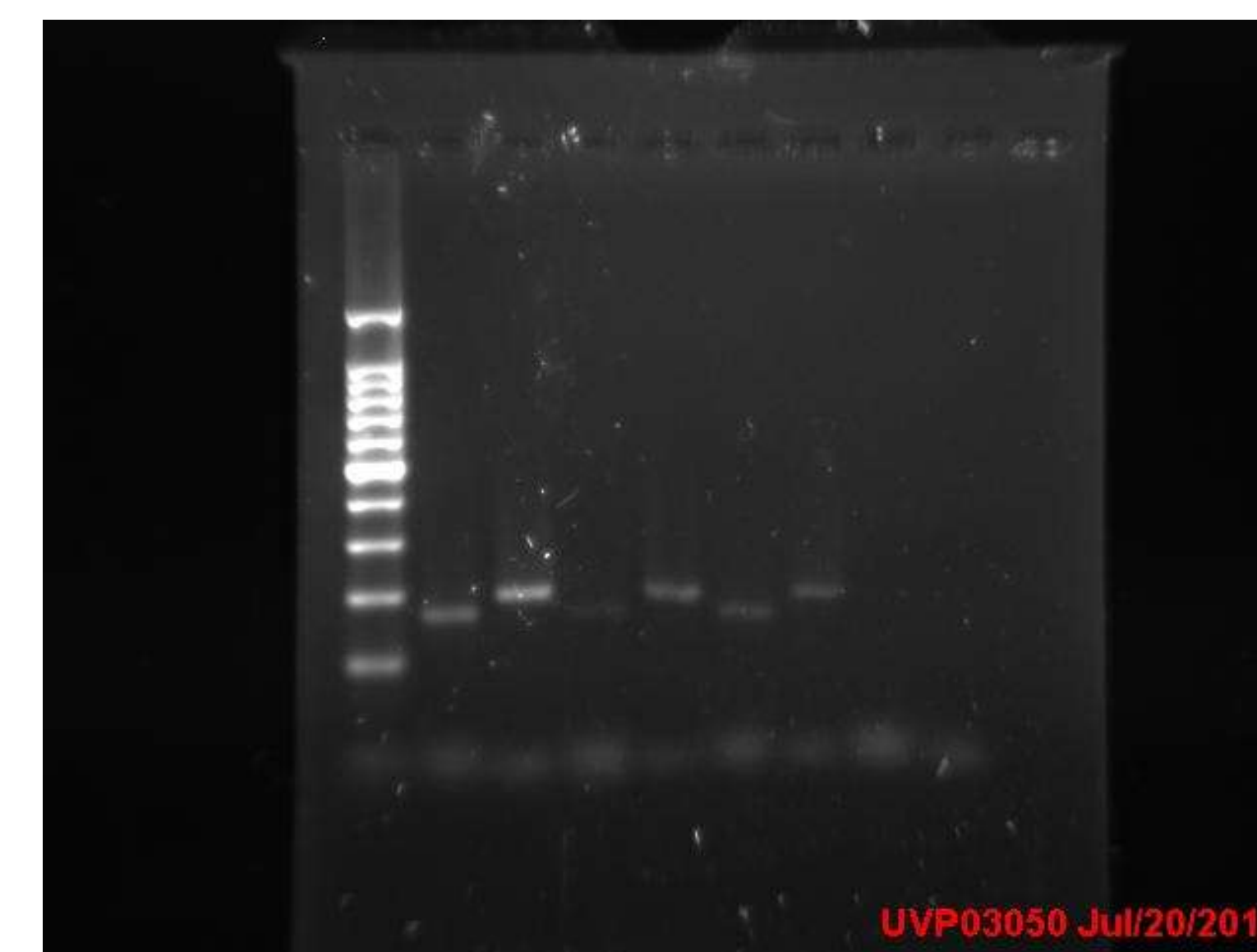


Figure 2: PCR results from U937 cells. 1 and 2 - positive control PCR reactions with histone H3 antibodyimmunoprecipitates using histone H3 and CaMKIV primers. 3 and 4 - RAR IPs PCR reactions using histone H3 and CaMKIV primers. 5 and 6 - negative control using no antibody with histone H3 and CaMKIV primers. 7 and 8 - did not contain DNA in the PCR sample.



Figure 3: PCR results from K562 cells. 1 and 2 - positive control PCR reactions with histone H3 antibodyimmunoprecipitates using histone H3 and CaMKIV primers. 3 and 4 - RAR IPs PCR reactions using histone H3 and CaMKIV primers. 5 and 6 - negative control using no antibody with histone H3 and CaMKIV primers. 7 and 8 - did not contain DNA in the PCR sample.

METHODS

Two myeloid leukemia cell lines, U937 and K562, were cultured in RPMI-1640 media. Cells were treated with 10% formaldehyde to a final concentration of 0.75% for 10 minutes to cross-link the proteins to the DNA. Glycine was then added to terminate the cross-linking reaction. Cells were then washed and resuspended in lysis buffer. The lysate was sonicated over a time course and the samples were analyzed on a 1.5% agarose gel to determine optimal conditions to obtain a desired fragment length of 200-800 base pairs. The 15 minutes and 10 minutes samples were chosen for U937 and K562 cells respectively. An immunoprecipitation (IP) was then performed using an Abcam ChIP kit and histone H3 and RAR-alpha antibodies. After the IP was performed the DNA was purified and a quantitative PCR was performed for analysis using histone and CaMKIV promoters.

CONCLUSION

Repression of CaMK4 transactivation by CaMKII has previously been proven in our lab using HEK 293 cells as the transfected target cell. The purpose of this study was to investigate whether this occurs in vivo, in leukemia cells. The U937 and K562 cell lines cannot be easily transfected, so a ChIP assay was utilized instead. Using the ChIP assay we established the baseline for RAR-alpha binding on CaMKIV promoter in the myeloid leukemia cell lines. The next step in this process is to inhibit CaMKII using KN-93 and to see how this effects CaMKIV expression

Determining the relationship between ubiquitin 1 and insulin-like growth factor 1 receptor in HEK 293T cells.

Jara Vega Velez, Levi Beverly, PhD
University of Louisville, Louisville, KY

Background

Ubiquitin1 (UBQLN1) is a protein that binds to ubiquitinated proteins and either takes the protein to the proteasome for degradation or protects the protein from degradation. UBQLN1 has been shown to play a role in protection and degradation of different proteins that may play a role in cancer. Insulin-like growth factor 1 receptor (IGF1R) activity has been linked to cancer and we have shown that IGF1R interacts with UBQLN1. IGF1R is a tyrosine kinase receptor that is activated by insulin-like growth factor 1 and insulin-like growth factor 2. Upon stimulation, IGF1R is auto-phosphorylated and begins a signaling cascade that is vital for cell proliferation and survival.

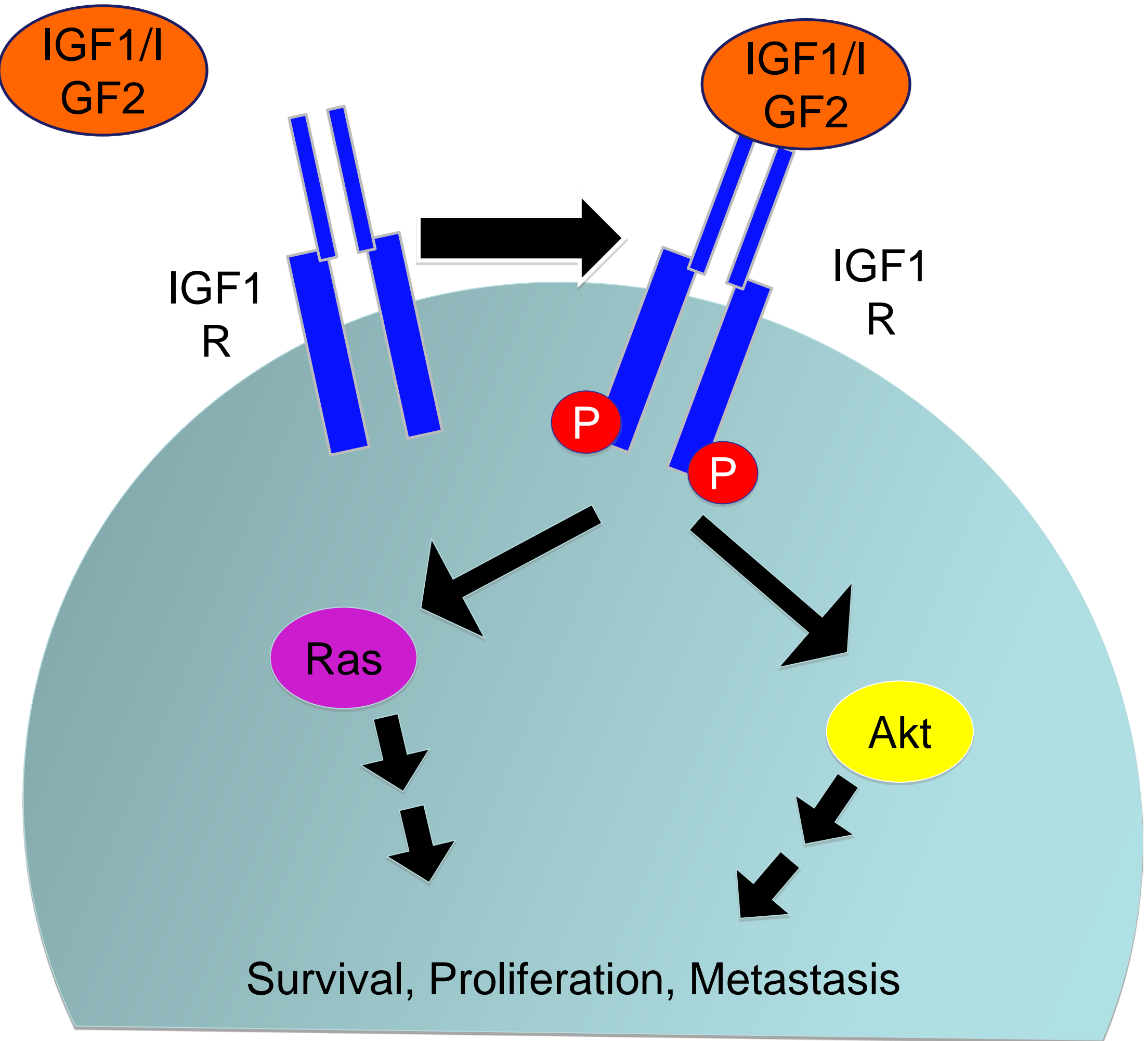


Figure 1: Schematic of IGF1R signaling

Objective

- The objectives of this experiment are:
- To confirm a relationship between UBQLN1 and IGF1R.
 - To determine the effect of UBQLN1 on the persistence of phosphorylated IGF1R in cells.
 - To compare the effects of UBQLN1 deletion mutants on the persistence of phosphorylated IGF1R in cells.

Results

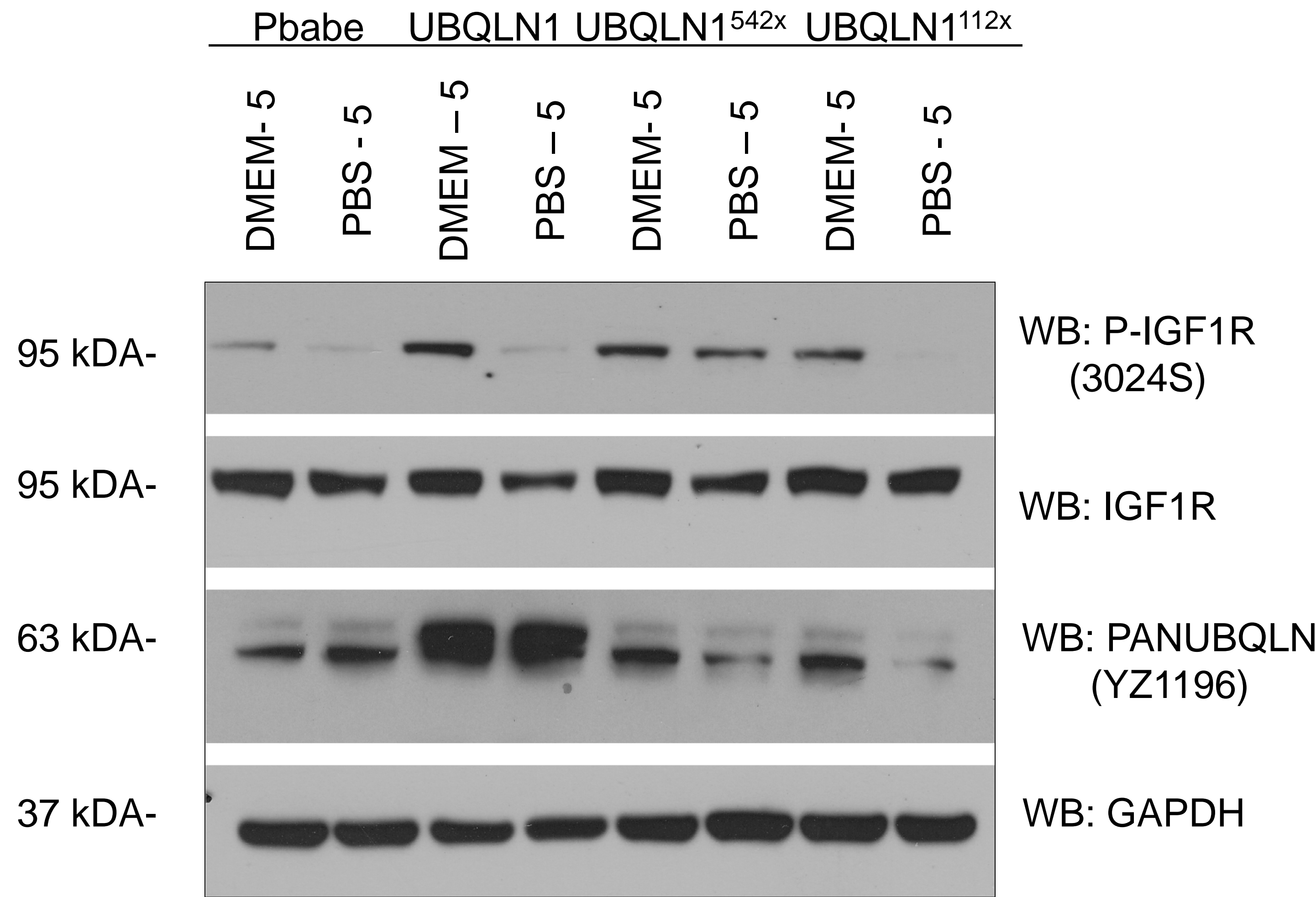


Figure 2: Cells treated with complete DMEM media or PBS for 5 minutes.

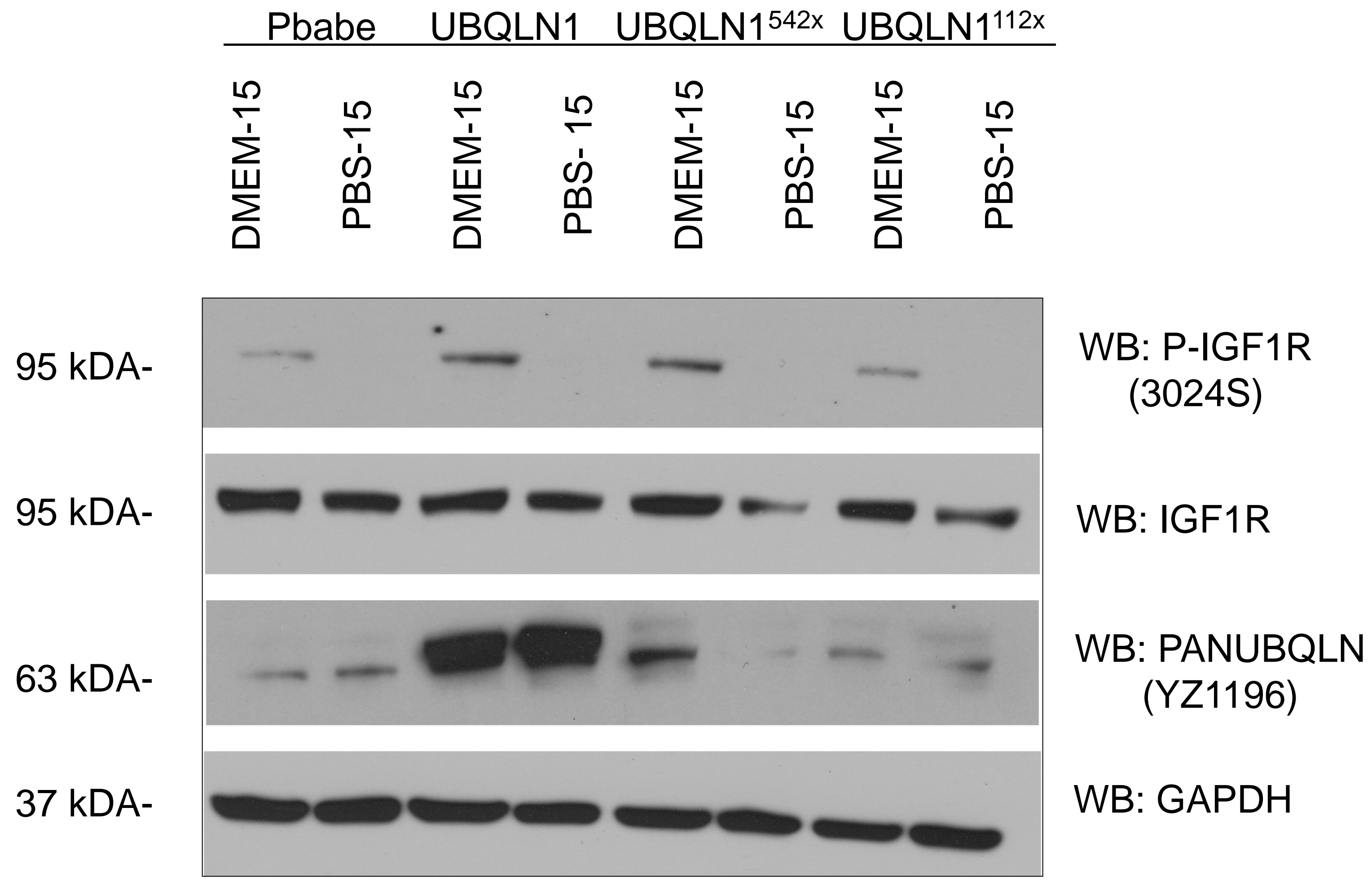


Figure 3: Cells treated with complete DMEM media or PBS for 15 minutes.

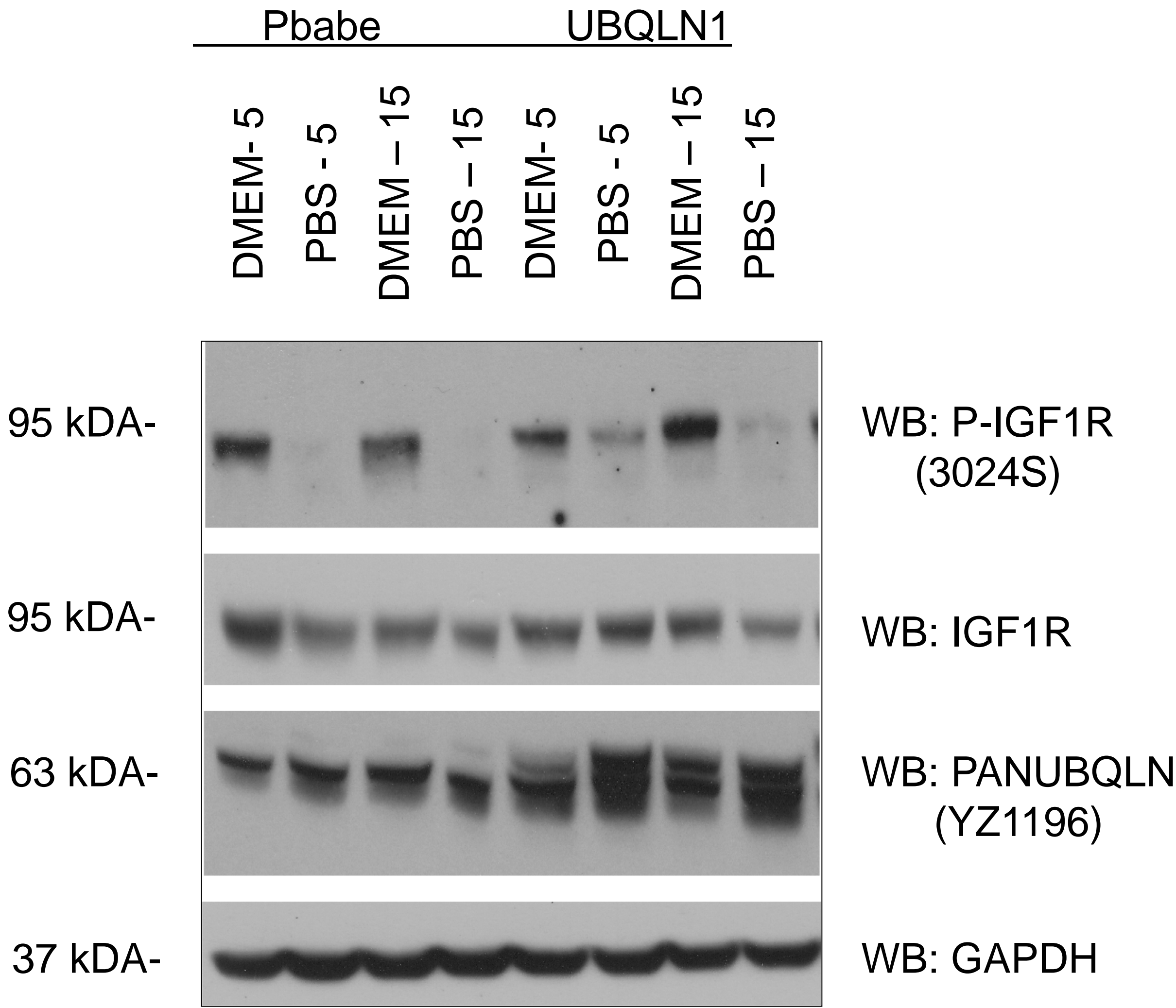


Figure 4: Cells treated with complete DMEM media or PBS for 5 or 15 minutes.

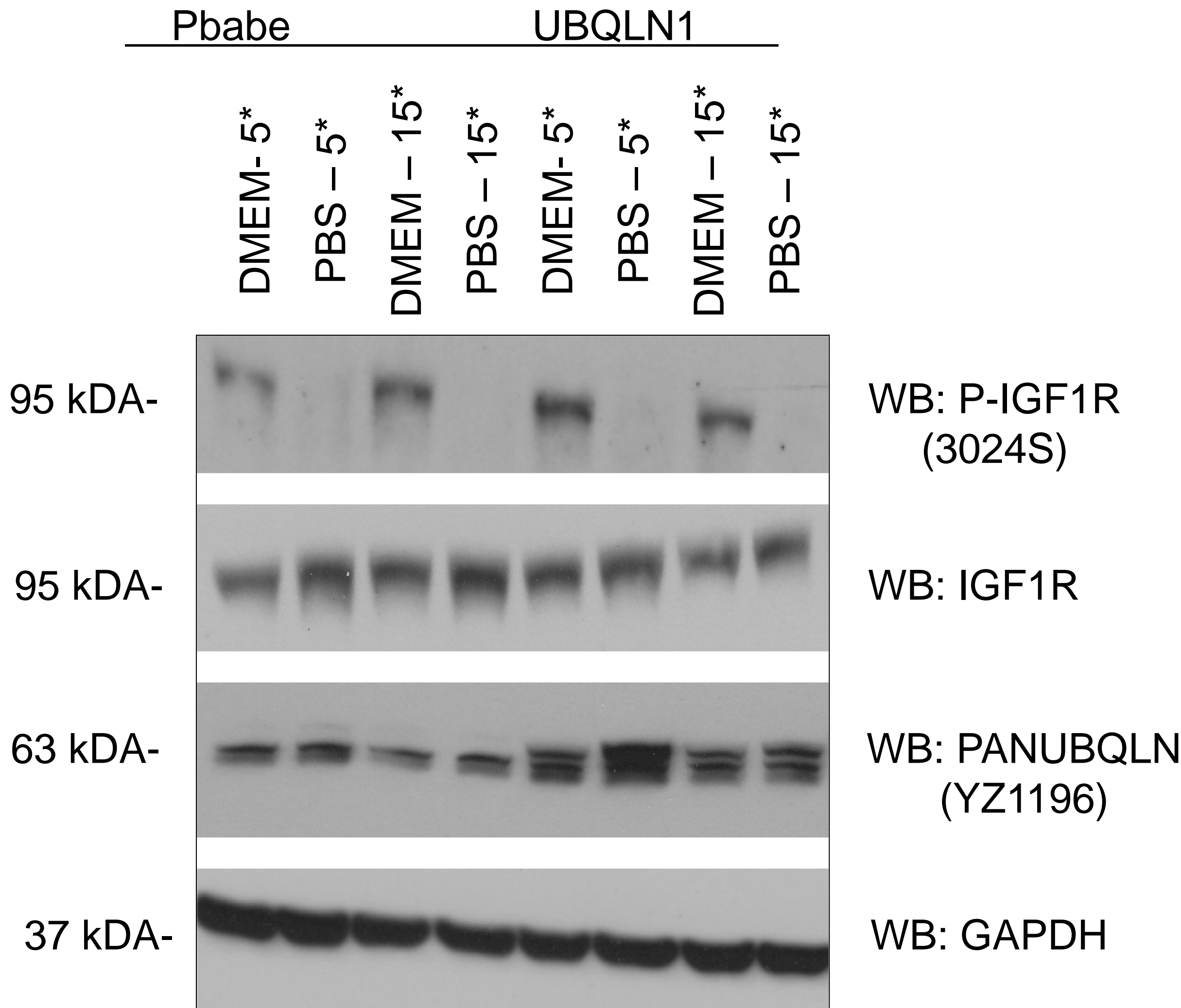


Figure 5: Cells serum-starved with PBS for 2 hours before treatment with complete DMEM media or PBS for 5 or 15 minutes.

Future endeavors

- Future experiments:
- To determine if effect of UBQLN1 on the persistence of phosphorylated IGF1R in cells starved only of growth factors compared to cells starved of growth factors and nutrients.
 - To determine when activation of IGF1R returns to cells after a period of starvation.
 - To determine if UBQLN1 plays a role in the return of IGF1R activation after a period of starvation.

Acknowledgments

We thank NCI R25 grant support, University of Louisville Cancer Education Program NIH/NCI (R25-CA134283), and Kosair Pediatric Cancer Program for funding support.